bioRxiv preprint doi: https://doi.org/10.1101/317339; this version posted May 8, 2018. The copyright holder for this preprint (which was not certified by peer review) is the author/funder, who has granted bioRxiv a license to display the preprint in perpetuity. It is made available under aCC-BY 4.0 International license.

BK channel inhibition by strong extracellular acidification

Yu Zhou, Xiao-Ming Xia and Christopher J. Lingle

Department of Anesthesiology, Washington University School of Medicine, St. Louis, Missouri 63110

Address for correspondence:

Yu Zhou
Washington University School of Medicine
Dept. Anesthesiology, Box 8054
St. Louis MO 63110
email: zhouy@wustl.edu

Christopher J. Lingle
Washington University School of Medicine
Dept. Anesthesiology, Box 8054
St. Louis MO 63110
phone: 314-362-8558
FAX: 314-362-8571
email: clingle@morpheus.wustl.edu

Running title: BK channel inhibition by extracellular H^+

Keywords: extracellular H+, K^+ channels, channel inhibition, BK channels, Slo1 channels

[1]Abbreviations used in this paper: BK, large conductance Ca^{2+}-activated K^+ channel

bioRxiv preprint doi: https://doi.org/10.1101/317339; this version posted May 8, 2018. The copyright holder for this preprint (which was not certified by peer review) is the author/funder, who has granted bioRxiv a license to display the preprint in perpetuity. It is made available under aCC-BY 4.0 International license.

Abstract

BK-type voltage- and Ca^{2+}-dependent K^+ channels are found in a wide range of cells and intracellular organelles. Among different loci, the composition of the extracellular microenvironment, including pH, may differ substantially. For example, it has been reported that BK channels are expressed in lysosomes with their extracellular side facing the strongly acidified lysosomal lumen (pH ~ 4.5). Here we show that BK activation is strongly and reversibly inhibited by extracellular H^+, with its conductance-voltage relationship shifted by more than +100 mV at pH_O 4. Our results reveal that this inhibition is mainly caused by H^+ inhibition of BK voltage-sensor (VSD) activation through three acidic residues on the extracellular side of BK VSD. Given that these key residues (D133, D147, D153) are highly conserved among members in the voltage-dependent cation channel superfamily, the mechanism underlying BK inhibition by extracellular acidification might also be applicable to other members in the family.

bioRxiv preprint doi: https://doi.org/10.1101/317339; this version posted May 8, 2018. The copyright holder for this preprint (which was not certified by peer review) is the author/funder, who has granted bioRxiv a license to display the preprint in perpetuity. It is made available under aCC-BY 4.0 International license.

Introduction

A hallmark of BK-type Ca^{2+} and voltage-activated K^+ channels is its dual regulation by two distinct physiological signals, Ca^{2+} and membrane potential (Latorre, Vergara, & Hidalgo, 1982; DiChiara & Reinhart, 1995; Horrigan & Aldrich, 2002). The key Ca^{2+} and voltage-sensing functions of the BK channel are embedded within the pore-forming BK α subunit and arise from interactions among three linked modules: a central pore-gate domain (PGD) that forms a K^+-selective ion permeation pathway, a transmembrane voltage-sensor domain (VSD) similar to that of the voltage-gate K^+ (Kv) channels (Ma, Lou, & Horrigan, 2006), and two regulator of conductance for K^+ (RCK) domains that form a cytosolic gating ring (CTD) to provide binding sites for intracellular ligands such as Ca^{2+} (Schreiber & Salkoff, 1997; Jiang, Pico, Cadene, Chait, & MacKinnon, 2001; Shi et al., 2002; Xia, Zeng, & Lingle, 2002; Xia, Zhang, & Lingle, 2004). Yet, despite the common Ca^{2+}- and voltage-sensing functions of all BK channels, BK channels typically exhibit considerable diversity in their functional properties among different loci of expression, e.g., in epithelial cells (Bailey et al., 2006; Grimm, Foutz, Brenner, & Sansom, 2007), smooth muscle (Robitaille, Garcia, Kaczorowski, & Charlton, 1993; Wellman & Nelson, 2003; Tanaka et al., 2004), neurons (Reinhart, Chung, Martin, Brautigan, & Levitan, 1991; Rosenblatt, Sun, Heller, & Hudspeth, 1997; Meredith et al., 2006), or even in various organelles (Singh et al., 2013; Li et al., 2014; Cao et al., 2015; Wang et al., 2017), thereby allowing them to play physiological roles suited to their particular location of expression. This diversity in function occurs despite the fact that only a single gene (KCa1.1; Kcnma1) encodes the pore-forming subunit of all BK channels. As a consequence, a critical part of understanding potential physiological roles of BK channels has been in uncovering the various factors and mechanisms that define cell-specific functional properties.

What factors contribute to defining the physiological roles of BK channels? At least some diversity in BK channel properties can arise from the stable cell-specific molecular composition of the BK channel complex, including alternative splicing of pore-forming α subunits (Tseng-Crank et al., 1994; Rosenblatt et al., 1997) and

bioRxiv preprint doi: https://doi.org/10.1101/317339; this version posted May 8, 2018. The copyright holder for this preprint (which was not certified by peer review) is the author/funder, who has granted bioRxiv a license to display the preprint in perpetuity. It is made available under aCC-BY 4.0 International license.

co-assembly with various accessory subunits (Wallner, Meera, & Toro, 1996; Xia, Ding, & Lingle, 1999; Brenner et al., 2000; Xia, Ding, Zeng, Duan, & Lingle, 2000; Brenner et al., 2005; Yan & Aldrich, 2010). BK channels can also be regulated on a shorter time scale by post-translational modifications such as phosphorylation (Tian et al., 2004; Tian, McClafferty, Chen, & Shipston, 2008) or even more briefly by binding of soluble factors to the BK channel complex, such as Ca^{2+} (Magleby & Pallotta, 1983; Schreiber & Salkoff, 1997; Xia et al., 2002), Mg^{2+}(Shi & Cui, 2001; Zhang, Solaro, & Lingle, 2001; Shi et al., 2002; Horrigan & Ma, 2008), heme (Tang et al., 2003; Horrigan, Heinemann, & Hoshi, 2005), carbon monoxide (Hou, Xu, Heinemann, & Hoshi, 2008b), or omega-3 fatty acid (Hoshi et al., 2013; Hoshi, Tian, Xu, Heinemann, & Hou, 2013). In the latter cases, modulation of BK activity appears to involve interactions with the regulatory factors to binding sites on the intracellular side of the BK channel. In contrast, despite the fact that the extracellular side of BK channels may be exposed to a wide range of microenvironments, little is known about how and even whether regulation of BK channels by extracellular soluble factors may occur.

One common potential extracellular regulator might be protons (H^+). Many BK channels are expressed in loci where they may experience extremely low extracellular pH ($pH_O < 5$). For example, BK channels regulate potassium secretion in the distal nephron (Bailey et al., 2006; Grimm et al., 2007), while urinary pH ranges from 6.5 to 7.5 daily in healthy people and may vary from 4.5 to 8.0 in pathological conditions (Wagner et al., 2004). Recently, BK channels were proposed to regulate Ca^{2+} release/refilling and membrane trafficking of lysosomes (Cao et al., 2015; Wang et al., 2017). In the case of lysosomes, the BK channels are oriented with their extracellular side exposed to a high concentration of H^+ in the lumen of the lysosome, the pH of which ranges from 4.2-4.7(Mindell, 2012; Xu & Ren, 2015). Some previous work on Kv1 (Claydon et al., 2000; Kwan, Fedida, & Kehl, 2006; Claydon et al., 2007; Claydon, Kehl, & Fedida, 2008) and KCNQ channels (Prole, Lima, & Marrion, 2003) establishes precedence that some Kv channels may be sensitive to pH_O in the pH range of 5-7, perhaps by effects on the pore region of these channels (Zhang, Kurata, Kehl, & Fedida, 2003; Claydon et al., 2008; Wang et

bioRxiv preprint doi: https://doi.org/10.1101/317339; this version posted May 8, 2018. The copyright holder for this preprint (which was not certified by peer review) is the author/funder, who has granted bioRxiv a license to display the preprint in perpetuity. It is made available under aCC-BY 4.0 International license.

al., 2017). However, the impact of pH_O below pH 5 such as that which might be found in the lumen of a lysosome has not been systematically examined in Kv channels.

In this study, we address the questions of whether BK channels is sensitive to changes in pH_O and what the underlying mechanism of pH_O regulation might be. We report a strong and reversible inhibition of BK channel function by extracellular H^+ beginning around pH_O 6. The primary effect of low pH_O on BK channel function is to inhibit the activation of the BK VSD. In addition, a moderate change in the closed-open equilibrium of the BK permeation gate in favor of closed states also contributes to inhibition induced by extracellular acidification. The combination of these two effects positively shifts the BK conductance-voltage (G-V) relationship by more than 100 mV at pH_O 4. We further show that three acidic residues on the extracellular side of the BK VSD are involved in such inhibition. Given the possible presence of BK channels in loci such as the kidney or lysosomes where the extracellular face of BK channels may be exposed to extremely acidic conditions, these results must be taken into account in regards to proper assessment of the potential physiological and pathological roles that BK channels may play in such loci. Furthermore, given that the three key residues identified in this study are highly conserved among members in the voltage-dependent cation channel superfamily, the mechanism underlying BK inhibition by strong extracellular acidification might also be applicable to Kv channels and other members in this family, some of which also perform their physiological function in extremely acidic environments (Heitzmann & Warth, 2007).

Results

BK channel activation is strongly inhibited at pH_O lower than 5.

Given the possibility that BK channels may be expressed in loci in which the normally extracellular side of BK channels is exposed to acidic conditions, here we have examined the impact of pH_O on BK channel function.

bioRxiv preprint doi: https://doi.org/10.1101/317339; this version posted May 8, 2018. The copyright holder for this preprint (which was not certified by peer review) is the author/funder, who has granted bioRxiv a license to display the preprint in perpetuity. It is made available under aCC-BY 4.0 International license.

Figure 1A shows macroscopic BK currents recorded from an outside-out patch perfusing in extracellular solutions at pH 7 (left), pH 4 (middle), and back to pH 7 (right). The amplitude of macroscopic BK current was reduced at pH_O 4, with reduction became increasingly apparent as the voltage is made more negative, for example, comparing moderate depolarization at +60 mV (Fig. 1A, red traces) to that at +160 mV (Fig. 1C, blue trace), or comparing the reduction in inward tails at -120 mV (Fig. 1A and B) to the reduction in outward current at +160 mV (Fig. 1C, blue trace). A previous study showed that neutralization of a highly conserved acidic residue (D292N) in the BK channel pore region reduces single channel conductance and induces an outward rectification in resulting BK channels (Haug et al., 2004). In a similar fashion, we observed that BK single channel conductance was reduced by ~50% at -120 mV and ~20% at +60 mV when pH_O was changed from 7 to 4 (Figure 1C). This change in single channel conductance can largely account for the reduction of maximum tail current at -120 mV (Figure 1B). However, it is also clear that the reduction of BK single channel conductance induced by extracellular acidification accounts for only a small portion of the changes in outward current amplitude over the physiologically relevant voltage range (e.g., the amplitude of macroscopic BK current at +60 mV was reduced by ~85% when pH_O was changed from 7 to 4). At more positive potentials, the amplitude of BK current at pH_O 4 was closer to that at pH_O 7. However, the reduction in macroscopic current amplitude with pH_O changed from 7 to 4 was greater than that in single channel conductance over all the voltages we examined. For example, the amplitude of current evoked by +160 mV pulse at pH_O 4 was only 0.72±0.02 (n = 6) of that at pH_O 7, while the BK single channel conductance at pH_O 4 was estimated to be 0.88 of that at pH_O 7 at the same voltage (Fig. 1C). Above results indicate that extracellular acidification strongly shifts the voltage-dependent gating of BK channel toward positive potential.

We therefore plotted the conductance-voltage (G-V) relationship for BK activation at a given pH_O normalized to the maximum conductance at that pH_O (Fig. 1D). This revealed that the G-V relationship was shifted toward positive potentials with increases in extracellular $[H^+]$. The BK half-activation potential (V_h) was shifted by more than +60 mV when pH_O was changed from 7 to 5 and was further shifted by another +70 mV at

bioRxiv preprint doi: https://doi.org/10.1101/317339; this version posted May 8, 2018. The copyright holder for this preprint (which was not certified by peer review) is the author/funder, who has granted bioRxiv a license to display the preprint in perpetuity. It is made available under aCC-BY 4.0 International license.

pH_O 4. With a gating shift of this magnitude, the P_O of BK did not reach maximum level even at +160 mV when pH_O was changed from 7 to 4 (Fig. 1D).

In addition to reduction in current amplitude, the kinetics of BK current was also significantly changed with elevation of extracellular $[H^+]$, with activation being much slower while deactivation being much faster at pH_O 4 than at pH_O 7 (Fig. 1A). These changes in channel kinetics are also consistent with the gating of BK channels shifted toward positive potentials by extracellular H^+. Importantly, the activation of BK channels remained low over the physiologically relevant voltage range of ±60 mV at pH_O 4 even with saturating $[Ca^{2+}]_{in}$ (Figure 1D). Therefore, the primary contributor to reduction in BK activation at pH_O 4.0 over these voltages is the shifted BK gating but not the reduction in single channel conductance. The gating shift induced by extracellular H^+ appeared to be independent of $[Ca^{2+}]_{in}$ as a comparable G-V shift was observed with 10 μM $[Ca^{2+}]_{in}$ (Figure 3C). It should be noted that even with a rather modest gating shift such as that induced by pH_O of 6 (~20mV), the resulting reduction in the BK channel current could still be sufficient to markedly alter the physiological function of BK channels.

The change of V_h induced by extracellular acidification is plotted against pH_O in Figure 1E. The approximate IC_{50} of pH_O-dependent BK G-V shift is pH 3.8, suggesting that acidic residue(s) on the extracellular side of the BK channel may be involved in this inhibition.

A change in the C-O equilibrium only accounts for a small portion of the gating shift induced by extracellular H^+

We next sought to address the question of the mechanistic basis for the rightward gating shift induced by extracellular protons. Extracellular H^+ might inhibit BK channel activation by several different mechanisms, including inhibition of either opening of the BK permeation gate or activation of the BK VSD. The modular design of BK channel protein and allosteric nature of BK channel gating make it possible to examine these possibilities separately. Previous studies suggest that extracellular acidification inhibits Kv1 channels by enhancing

bioRxiv preprint doi: https://doi.org/10.1101/317339; this version posted May 8, 2018. The copyright holder for this preprint (which was not certified by peer review) is the author/funder, who has granted bioRxiv a license to display the preprint in perpetuity. It is made available under aCC-BY 4.0 International license.

inactivation in the pore domain of these channels (Claydon et al., 2007; Kwan et al., 2006; Trapani and Korn, 2003; Zhang et al., 2003). Therefore, we started by examining the effects of extracellular acidification on the closed-open equilibrium in the BK pore region. To do this, we recorded BK single channel currents at negative potentials (-100 mV) where VSDs of BK channel are largely in resting states. A change in limiting open probability times the number of BK channels (limiting nP_O) determined from such recordings reflects a change in the C-O equilibrium of the BK pore gate (Horrigan, Cui, & Aldrich, 1999). As shown in Figure 2A, the limiting nP_O of BK channels was moderately reduced when pH_O was changed from 7 to 4. The average limiting nP_O of BK channels at pH_O 4 was 0.31 of that at pH_O 7, indicating that the C-O equilibrium constant *L* of BK channels was reduced by about 2-fold with extracellular acidification at pH_O 4. To evaluate the impact of such reduction of *L* on BK channel gating we simulated G-V relationships using the Horrigan-Aldrich (H-A) model with the zero voltage C-O equilibrium constant (L_0) scaled down from one published value of 1×10^{-6} (Horrigan & Aldrich, 2002). As shown in Figure 2B and C, G-V curves simulated with L_0 reduced by 2-fold are only predicted to be positively shifted by about 20-mV from the control G-V, much less than the gating shift observed in our experiments. The H-A simulation also showed that a 1000-fold reduction in L_0 was required to reproduce the observed G-V shift if the only effect of extracellular H^+ was to alter the C-O equilibrium of BK channel (Figure 2B, C). Therefore, a change in the C-O equilibrium cannot fully account for the gating shift induced by extracellular acidification.

Gating current measurement shows that activation of BK VSD is strongly inhibited by extracellular H^+

To directly determine the effect of extracellular H^+ on the function of the BK VSD, we compared the fast components of BK channel gating current (I_{gfast}) recorded from giant outside-out patches at pH_O 7 and 4 (Figure 3A). The I_{gfast}, which reflects the movement of the BK VSD in closed channels, was isolated by fitting the first 100 μs of I_{gON} with an exponential function (Horrigan & Aldrich, 1999; Horrigan & Aldrich, 2002). The fast charge movement associated with VSD activation (Q_{fast}) was then determined by integration under the exponential fit.

bioRxiv preprint doi: https://doi.org/10.1101/317339; this version posted May 8, 2018. The copyright holder for this preprint (which was not certified by peer review) is the author/funder, who has granted bioRxiv a license to display the preprint in perpetuity. It is made available under aCC-BY 4.0 International license.

The Boltzmann fit of the Q_{fast}-V relationship shows that the V_h of BK VSD activation was positively shifted from 190 mV to 309 mV when pH_O was changed from 7 to 4 (Figure 3B). In addition, the slope of Q_{fast}-V relationship was reduced from 0.46*e* to 0.39*e*, indicating that the effective gating charge associated with BK VSD movement was moderately reduced by extracellular acidification. Figure 3C shows the G-V curves of BK channels at pH_O 7 and 4 with 10 μM $[Ca^{2+}]_{in}$. We first fit the G-V at pH_O 7 using the H-A model with V_{hC} (half-activating voltage of BK VSD in a closed channel) and z_J (partial charge associated with the BK VSD resting-activated equilibrium constant *J*) fixed at the values determined from the Q_{fast}-V relationship at pH_O 7 and published values (Horrigan & Aldrich, 2002) as initial guesses for all other parameters (Figure 3C, black line). Then we calculated the predicted BK G-V curves at pH_O 4 based on our measured changes either in L_0, in V_{hC} and z_J, or both. The calculated GV based on a two-fold reduction of L_0 only positively shifted the G-V (Figure 3C, cyan line) by less than 20 mV from the G-V at pH 7, while the GV calculated based on changes of BK VSD activation (V_{hC} increased from 190 mV to 309 mV, z_J reduced by 15%) along with the two-fold reduction in L_0 reasonably reproduced the gating shift induced by extracellular acidification at pH 4 (Figure 3C, red line). Therefore, the primary effect of extracellular acidification on BK channels is to inhibit BK VSD activation.

Three acidic residues on the extracellular side of BK VSD are involved in BK inhibition by extracellular H^+

The IC_{50} for the BK gating shift by extracellular H^+ is around pH 4 (Figure 1C), suggesting the involvement of acidic residues in BK inhibition by extracellular acidification. There are eight acidic residues on the extracellular side of each BK α-subunit, with four (D133, E139, D147, D153) in the VSD and the other four (E257, E264, E276, D292) in the PGD (Figure 4A). A multiple sequence alignment in the VSDs of different members of the voltage-dependent cation channel superfamily shows that the acidic residues in the VSD are largely conserved among these channels, with all four residues conserved between BK and Kv channels. For the four acidic residues in the BK PGD, only the two in the pore-loop (E276 and D292) are conserved between BK and Kv

bioRxiv preprint doi: https://doi.org/10.1101/317339; this version posted May 8, 2018. The copyright holder for this preprint (which was not certified by peer review) is the author/funder, who has granted bioRxiv a license to display the preprint in perpetuity. It is made available under aCC-BY 4.0 International license.

channels (Figure 4B). It should be mentioned that D292, a highly conserved residue among most K channels, has been systemically studied in human BK (hSlo1) channels in a previous study, which showed that the G-V of hSlo1 D292N is only moderately shifted toward positive potentials when compared with that of WT channels (Haug, Olcese, Toro, & Stefani, 2004). Therefore, it is unlikely that the large gating shift of BK channels that is induced by extracellular acidification would be mainly caused by reduced side chain charge of D292 at low pH_O. In the current study, we individually replaced seven other acidic residues (D133, E139, D147, D153, E257, E264, E276) with alanine and examined sensitivity of the resulting mutants to extracellular H^+. Consistent with the result that extracellular H^+ positively shifts the gating of BK channels mainly by inhibition of BK VSD activation, all three alanine substitutions that induced a significant reduction in the pH_O-dependent gating shift are in the BK VSD (D133A, D147A, D153A).

Among these three key residues, alanine-substitution of D153 had the greatest effect on the pH_O-dependent gating shift. As shown in Figure 5A, the activation and deactivation kinetics of D153A current at pH_O 4 were not significantly different from that at pH_O 7, even though the amplitude of the current was moderately reduced mostly due to a reduction of single channel conductance at pH_O 4. In accordance with this, the G-V curves of D153A were shifted by less than 10 mV when pH_O was changed from 7 to 4 (Figure 5B). Correspondingly, for D153A the change in gating equilibrium free energy by extracellular acidification at pH_O 4 ($\Delta G_0^{pH}=G_0^{pH4}-G_0^{pH7}=z^{pH4}FV_h^{pH4}-z^{pH4}FV_h^{pH7}$) was only 0.4 kCal/mol (Figure 5I). As a comparison, the same change of pH_O increased the gating equilibrium free energy of wild type (WT) BK channels by about 2.3 kCal/mol. This result shows that D153 is critical for BK inhibition by extracellular H^+.

In addition to D153A, alanine-substitution of D133 or D147 also significantly reduced the gating shifts induced by extracellular acidification, even though neither mutation was as effective as D153A in abolishing the pH_O-dependent gating shift. For D133A, changing pH_O from 7 to 4 still permitted a G-V shift of about +50-mV (Figure 5C and D), while for D147A, the same extracellular acidification shifted the G-V by more than +60-mV

bioRxiv preprint doi: https://doi.org/10.1101/317339; this version posted May 8, 2018. The copyright holder for this preprint (which was not certified by peer review) is the author/funder, who has granted bioRxiv a license to display the preprint in perpetuity. It is made available under aCC-BY 4.0 International license.

(Figure 5E and F). Despite the weaker effects of these mutations relative to D153A, both mutations reduced ΔG_0^{pH} by more than 1 kCal/mol (Figure 5I), indicating that both aspartates do contribute to BK inhibition by extracellular acidification. Double alanine-substitution of D133 and D147 (D133A/D147A) further reduced the magnitude of the pH_O-dependent gating shift. The G-V curve of this double mutant was shifted by less than +25 mV when pH_O was changed from 7 to 4 (Figure 5G and H). The coupling energy between D133 and D147 can be calculated using double-cycle mutation analysis (Yifrach & MacKinnon, 2002) as: $[(\Delta G_0^{pH}{}_{WT} - \Delta G_0^{pH}{}_{D133A})-(\Delta G_0^{pH}{}_{D147A} - \Delta G_0^{pH}{}_{D133AD147A})] = 0.66$ kCal/mol, indicating that these two acidic residues should contribute largely energetically independent effects in producing BK inhibition by extracellular acidification.

By comparing the G-Vs of the above mutants at pH_O 7 with that of WT channels it can be noticed that alanine-substitution at these key sites also induced positive gating shifts. In Figure 5J the change of gating equilibrium free energy by alanine-substitution at pH7 ($\Delta G_0^{MUT}=G_0^{MUT}-G_0^{WT}$) is plotted against ΔG_0^{pH}. From this plot it is clear that ΔG_0^{MUT} and ΔG_0^{pH} are inversely related, indicating that alanine-substitution of the three key acidic residues and extracellular acidification shift the gating of BK channels by a common mechanism.

Discussion

In this study we describe a strong and reversible inhibitory effect of extracellular H^+ on BK channel activation at pH_O below 6, with particularly profound effects at pH 5 and 4. This inhibition involves multiple mechanisms, with inhibition of BK VSD activation as the primary mechanism. In addition to inhibition of BK VSD, extracellular H^+ also induces a moderate change in the C-O equilibrium of channel activation favoring the closed conformation. There is also a direct pore inhibition by extracellular protons, but this effect will be of minor impact in the face of the large gating shifts. The combination of the effects on VSD activation and C-O equilibrium shifts the G-V relationship of BK toward positive potentials by more than 100 mV at pH_O 4. As a result, the activity of BK channels is low in physiological voltage ranges when the channels are exposed to a strongly acidified extracellular environment even with saturating intracellular Ca^{2+}. We further show that

bioRxiv preprint doi: https://doi.org/10.1101/317339; this version posted May 8, 2018. The copyright holder for this preprint (which was not certified by peer review) is the author/funder, who has granted bioRxiv a license to display the preprint in perpetuity. It is made available under aCC-BY 4.0 International license.

alanine-substitution of three acidic residues in the extracellular side of BK VSD reduces the gating shift caused by extracellular acidification, suggesting that H^+ inhibits BK channel activation mainly by reducing the charge of these acidic residues. Since these three acidic residues are highly conserved among voltage-dependent K^+ channels, inhibition of VSD activation could be a universal mechanism for extracellular H^+ to regulate the activity of voltage-dependent ion channels that may be exposed to acidic environments.

Relation to previous studies and structural implications. Some previous studies have examined aspects of the effect of extracellular acidification on Kv channels, usually at more moderate pHs above 5.0 (Deutsch & Lee, 1989; Horrigan & Aldrich, 1999; Claydon et al., 2000; Prole et al., 2003; Kwan et al., 2006; Claydon et al., 2007; Claydon et al., 2008). At such concentrations, extracellular H^+ has been observed to act primarily in the pore region of these channels to reduce current amplitude. For example, pH_O 5.9 inhibits Kv 1.5 channels by accelerating entry of open channels into P/C-type inactivation and by stabilizing closed channels in closed-inactivated states (Claydon et al., 2008). In the current study, we show that strong acidification at pHs lower than 5 induces additional inhibition in the BK VSD, most likely by reducing the side chain charges of three key acidic residues on the extracellular side of BK VSD. Given that these three residues are highly conserved between BK and Kv channels, it is reasonable to assume that the activation of Kv VSD could also be inhibited by such strong extracellular acidification. Indeed, it has been shown that the G-V and Q-V relationships of Kv1.5 were also significantly shifted toward positive potentials at pH_O 5 or lower (Claydon et al., 2007).

Among the three key residues involved in BK inhibition by extracellular H^+, D153 in the S2 of BK VSD appears to be the most important one as D153A almost completely abolishes the BK gating shift induced by extracellular acidification. D153 was identified as a potential voltage-sensing residue for BK channels by a previous mutagenesis analysis of the BK VSD (Ma et al., 2006). In this work the authors analyzed BK ionic current within the framework of the H-A model to show that substitution of D153 by cysteine reduces the z_j of BK channels by 40%. In agreement with this result, by examining gating currents recorded at different pH_Os, we

bioRxiv preprint doi: https://doi.org/10.1101/317339; this version posted May 8, 2018. The copyright holder for this preprint (which was not certified by peer review) is the author/funder, who has granted bioRxiv a license to display the preprint in perpetuity. It is made available under aCC-BY 4.0 International license.

found that the z_j of BK channels was reduced by extracellular H^+ (Figure 3B). It should be noted that the z_j of BK channels was only reduced by 15% at pH_O 4, suggesting that the side chain of D153 may still be partially charged at pH_O 4. In accordance with this, the BK gating shift induced by changing pH_O from 7 to 4 was less than that induced by D153A mutation (Figure 5B).

To understand the role of D153 in BK VSD activation, we generated a pair of homologous mSlo1 structures using two recently published Aplysia BK (aBK) channel cryo-EM structures as templates (Tao, Hite, & MacKinnon, 2017; Hite, Tao, & MacKinnon, 2017). The one based on the structure solved in the presence of saturating intracellular Ca^{2+} and Mg^{2+} is termed "liganded" and the other based on the structure solved in the absence of intracellular divalent cation is termed "metal-free". Figure 6A shows the VSDs of these two mSlo1 structures superimposed by their pore-loops. It can be seen that D153 is located at the bottom of a crevice on the extracellular end of the BK VSD, with little displacement (< 1 Å) of D153 between these two structures. As a comparison, the side chain of R213, another primary voltage sensing residue located in the BK S4 (Ma et al., 2006) is shifted toward the extracellular side by more than 3.5 Å in the liganded structure. Based on the functional importance of the free carboxyls of D153 in gating, we searched for potential hydrogen bonds that might involve the side chain of D153 in the two mSlo1 structures. The result shows that D153 may form candidate hydrogen bonds with several different S4 residues in the two structures. In the metal-free structure, one of the carboxyl oxygens in the side chain of D153 is within the hydrogen-bonding distance with the δ-nitrogen of R207 (3.1 Å, Figure 6B), while in the liganded structure both carboxyl oxygens of D153 are aligned with the two ω-nitrogens of R210 for potentially strong hydrogen bonding (Figure 6C). These observations are in accordance with the result from a previous study of BK inhibition by extracellular Cu^{2+}, which shows that both D153 and R207 are required for Cu^{2+} coordination in the BK VSD in resting states (Ma, Wong, & Horrigan, 2008). Thus, it is conceivable that D153 might interact with various basic residues in BK S4 to stabilize the VSD in particular transitional conformations on the pathway to activation. If this was true, then extracellular acidification could inhibit BK VSD activation by weakening such interactions. Indeed, previous work shows that

bioRxiv preprint doi: https://doi.org/10.1101/317339; this version posted May 8, 2018. The copyright holder for this preprint (which was not certified by peer review) is the author/funder, who has granted bioRxiv a license to display the preprint in perpetuity. It is made available under aCC-BY 4.0 International license.

residues with opposite charges placed at *Shaker* 283 and *Shaker* 368 (homologous to mSlo1 R210) can stabilize the VSD of the resulting *Shaker* channel in a partially active conformation (Tiwari-Woodruff, Lin, Schulteis, & Papazian, 2000).

In addition to D153, we also identified two other acidic residues (D133 and D147) that are important for BK inhibition by extracellular H^+ and therefore important for the function of the BK VSD. Replacing each of these two asparates with alanine causes a significant reduction in the pH_O-dependent gating shift, while the impact of the double alanine-substitution (D133AD147A) on the gating shift induced by extracellular acidification is comparable to that of D153A. D133 and D147 are more exposed to the extracellular environment than D153 in both mSlo1 structures (Figure 6A). For D133 in the S1 helix of BK VSD, there is little change in position between the two structures. The side chain of D133 is close to R207 in both mSlo1 structures (Figure 6 D-E), indicating that D133 may also form important interactions with S4 residues to stabilize BK VSD. Interestingly, D133 is also involved in Cu^{2+} coordination with the BK VSD (Ma et al., 2008). The lack of change in distance between D133 and R207 in the two mSlo1 structures indicates that either the state-dependence of Cu^{2+}-VSD coordination is largely determined by the distance between D153 and R207, or the conformation captured by the liganded structure represents a partially activated VSD state. For D147, a large displacement is observed between the two structures, which is not totally unexpected as D147 is in the flexible S1-S2 linker. However, this displacement is largely horizontal. Thus, D147 remains on the surface of the BK VSD in both structures. Unlike that of D153 and D133, the side chain of D147 is not close to any residue with potential for strong interaction in the two mSlo1 structure, indicating that D147 may not contribute to VSD activation by interacting with other residues to stabilize transitional conformations during VSD activation. Instead, D147 may participate in BK VSD activation by altering local electric field.

Physiological implications. As an ion channel with great physiological importance, the BK channel is a popular subject for research on ion channel regulation. Whereas regulation of BK channels by cytosolic factors

bioRxiv preprint doi: https://doi.org/10.1101/317339; this version posted May 8, 2018. The copyright holder for this preprint (which was not certified by peer review) is the author/funder, who has granted bioRxiv a license to display the preprint in perpetuity. It is made available under aCC-BY 4.0 International license.

has been extensively studied (Hou, Heinemann, & Hoshi, 2009), much less is known about how physiological signals may regulate BK channels on the extracellular face of the BK channel. Two recent studies suggest that BK channels are ubiquitously expressed in lysosomal membranes in both excitable and non-excitable cells (Cao et al., 2015; Wang et al., 2017). The results from these studies suggest that lysosomal BK channels are functionally coupled with the lysosomal Ca^{2+}-permeable channel TRPML1 to regulate lysosomal Ca^{2+} release/refilling, which is a key process underlying lysosomal physiology (Xu & Ren, 2015). Since the extracellular side of the lysosomal BK channel is expected to be exposed to the acidic environment of the lysosome lumen, the basal activity of the lysosomal BK channel is expected to be low. However, it should be noted that lysosomal pH is highly heterogeneous, with the luminal pH of some primary lysosomes close to 7 (Johnson, Ostrowski, Jaumouille, & Grinstein, 2016; Bright, Davis, & Luzio, 2016). Therefore, it is conceivable that the activity of lysosomal BK channels might be regulated by lysosomal luminal pH. Interestingly, BK channels are also sensitive to intracellular H^+, which mimics the effect of Ca^{2+}-binding in the BK RCK1 domain (Avdonin, Tang, & Hoshi, 2003; Hou, Xu, Heinemann, & Hoshi, 2008a). Thus, intracellular H^+ may enhance the activity of BK channels in the absence of intracellular Ca^{2+}, while during elevations of intracellular Ca^{2+}, intracellular H^+ may inhibit BK channel activity (Cook, Ikeuchi, & Fujimoto, 1984; Christensen & Zeuthen, 1987; Schubert, Krien, & Gagov, 2001; Guarina, Vandael, Carabelli, & Carbone, 2017), presumably by interfering with Ca^{2+}-binding. In any case, it is clear that the present results require that any consideration of the role of BK channels in lysosomes must take into account its regulation by luminal pH.

In excitable cells, might changes in extracellular pH affect excitability? Although it seems unlikely that neurons will be exposed to pH as low as those required to inhibit BK channels in the presence study, a recent study has observed that BK channels in mouse chromaffin cells (MCC) are inhibited by extracellular H^+ (Guarina et al., 2017). The mechanism underlying this inhibition appears to be different from that described in the current study for two reasons: first, the IC_{50} of MCC BK inhibition by extracellular H^+ is 0.1 μM (pH 7), which is lower than what we observed in our experiment (52 μM/pH 4.3). Second, the onset (> 30-s) and recovery (~3-min) of MCC

bioRxiv preprint doi: https://doi.org/10.1101/317339; this version posted May 8, 2018. The copyright holder for this preprint (which was not certified by peer review) is the author/funder, who has granted bioRxiv a license to display the preprint in perpetuity. It is made available under aCC-BY 4.0 International license.

BK inhibition by extracellular H^+ is much slower than that of the inhibition described here (< 1-s for both onset and recovery). Based on the IC_{50} and the time course of MCC BK inhibition by extracellular H^+, it seems likely that at least some of the BK inhibition observed in CCs with extracellular acidification may reflect the time course of intracellular acidification induced from elevation of extracellular $[H^+]$.

Materials and Methods

General methods. Oocyte preparation, handling of RNA, and electrophysiological methods used here were identical to those described in other papers from this laboratory (Zhang et al., 2001; Zhou, Tang, Xia, & Lingle, 2010; Zhou & Lingle, 2014) . In brief, the mouse homologue of BK channels (mSlo1, mKCa1.1) were expressed in *Xenopus* oocytes by RNA injection. All BK ionic and gating currents presented in the current work were recorded from excised patches in the outside-out configuration (Hamill, Marty, Neher, Sakmann, & Sigworth, 1981). The pipette resistance for ionic current recording was typically 1-2 MΩ after heat polishing. The pipette solution (bathing the cytoplasmic face of patch membranes) contained (in mM): 140 K-methanesulfonate (K-MES), 20 KOH, 10 HEPES, with pH adjusted to 7.0 by methanesulfonic acid. 5 mM EGTA was included in 0 Ca^{2+} pipette solution. For 10 μM Ca^{2+} pipette solution, 5 mM HEDTA was used as Ca^{2+} buffer. For 300 μM Ca^{2+} pipette solution, no Ca^{2+} buffer was added. 10 μM Ca^{2+} solution was prepared by adding 1M Ca-MES stock solution to obtain the desired $[Ca^{2+}]$, as defined with a Ca^{2+}-sensitive electrode calibrated with commercial Ca^{2+} solutions (WPI, Sarasota, FL). Gigaohm seals were formed while the oocytes were bathed in frog Ringer (in mM, 115 NaCl, 2.5 KCl, 1.8 $CaCl_2$, 10 HEPES, pH 7.4). Following patch excision, the pipette tip was moved into flowing test solutions. Solution exchange at the tip of recording pipette was accomplished with an SF-77B fast perfusion stepper system (Warner Instruments, Hamden, CT). The composition of the solution used to bath the extracellular membrane face was (in mM) 140 KMES, 20 KOH, 2 $MgCl_2$, 10 HEPES, with pH adjusted to desired concentration by methanesulfonic acid.

bioRxiv preprint doi: https://doi.org/10.1101/317339; this version posted May 8, 2018. The copyright holder for this preprint (which was not certified by peer review) is the author/funder, who has granted bioRxiv a license to display the preprint in perpetuity. It is made available under aCC-BY 4.0 International license.

Gating current was recorded from outside-out macropatches using pipettes with tip diameters of 10-20 μm. The internal pipette solution contained (mM): 141 NMDG, 135 methanesulfonic acid, 10 HEPES, and 5 EGTA, pH 7.0. The external solution contained (mM): 127 tetraethylammonium hydroxide, 125 methanesulfonic acid, 2 $MgCl_2$, and 10 HEPES, with pH adjusted to desired value using methanesulfonic acid. Both voltage command and current output were filtered at 20 kHz with 8-pole Bessel filters (Frequency Devices) to avoid saturation by fast capacitive transients (Horrigan & Aldrich, 1999). Gating currents were sampled at 100 kHz. A P/-6 protocol was used for leak subtraction from a holding potential of -120 mV (Armstrong & Bezanilla, 1974).

All experiments were performed at room temperature (~22-25°C). pH of extracellular solutions was checked daily before recording. All chemicals were purchased from Sigma-Aldrich.

Data analysis. The G-V relationship of BK channels was determined from tail currents measured 150 μs after repolarization to -120 mV. G-V curves were fit by a Boltzmann function of the form of

$G(V) = \frac{G_{\max}}{1+\exp(-z(V-V_h)/kt)}$, where G_{max} is maximal conductance, z is apparent voltage-dependence in units of elementary charge, V_h is the voltage of half-maximal activation, and k and T have their usual physical meanings. The Horrigan-Aldrich (H-A) model (Horrigan & Aldrich, 2002) was also used for G-V curve fitting and simulation. This model describes the gating of BK channel as three sets of allosterically coupled conformational changes reflecting the three functional modules of a BK channel: 1. the closed-open equilibrium in the PGD (C-O, equilibrium constant $L = L_0\exp(z_L V/kT)$, where L_0 and z_L are the zero voltage value of L and its partial charge, respectively), 2. resting-activated equilibrium in the VSD (R-A, equilibrium constant $J = J_0\exp(z_J V/kT) = \exp(z_J(V-V_{hC})/kT)$, where J_0 and z_J are the zero voltage value of J and its partial charge, respectively, while V_{hC} is the half-activating voltage of BK VSD in a closed channel), and 3. Ca^{2+} binding in the CTD (X-X•Ca^{2+}, binding constant K). The coupling between PGD and VSD is represented by an allosteric factor D such that L increases D-fold with the activation of each VSD. Similarly, interactions of Ca^{2+}-binding with PGD and VSD are represented by allosteric

bioRxiv preprint doi: https://doi.org/10.1101/317339; this version posted May 8, 2018. The copyright holder for this preprint (which was not certified by peer review) is the author/funder, who has granted bioRxiv a license to display the preprint in perpetuity. It is made available under aCC-BY 4.0 International license.

factors C and E, respectively. This model defines the steady-state open probability (P_O) of BK channel as

$$P_O = \frac{L(1+KC+JD+JKCDE)^4}{L(1+KC+JD+JKCDE)^4+(1+K+J+JKE)^4}.$$

The voltage-dependent change of BK single channel current induced by extracellular acidification was fit by the Woodhull model (Woodhull, 1973): $\frac{i_{pH4}}{i_{pH7}} = \frac{k_{d0}+10^{-7}\exp(-\delta zVF/RT)}{k_{d0}+10^{-4}\exp(-\delta zVF/RT)}$, in which i_{pH4} and i_{pH7} are the unitary current at pH_O 4 and pH_O 7, respectively, k_{d0} is the dissociation constant of blocking ion at 0 mV, V is the transmembrane potential, δ is the fraction of the membrane potential at the blocking ion binding site, and z is the valence of the blocking ion (z = 1e for H^+). F, R and T have their usual physical meanings.

Open probability times the number of BK channels (nP_O) at negative potentials (limiting nP_O) was determined from single channel traces using the threshold-based Event Detection mode in Clampfit 9.2 (Molecular Device). Homologous structures of mSlo1 were built in MODELLER 9 (Sali & Blundell, 1993) using the Cryo-EM structures of the Aplysia BK channel as templates (Tao et al., 2017; Hite et al., 2017). Structure analysis and structure image preparation were accomplished using UCSF Chimera (Pettersen et al., 2004). Data were analyzed using OriginPro 7.5 (OriginLab Corporation) or programs developed in this laboratory.

bioRxiv preprint doi: https://doi.org/10.1101/317339; this version posted May 8, 2018. The copyright holder for this preprint (which was not certified by peer review) is the author/funder, who has granted bioRxiv a license to display the preprint in perpetuity. It is made available under aCC-BY 4.0 International license.

Figures

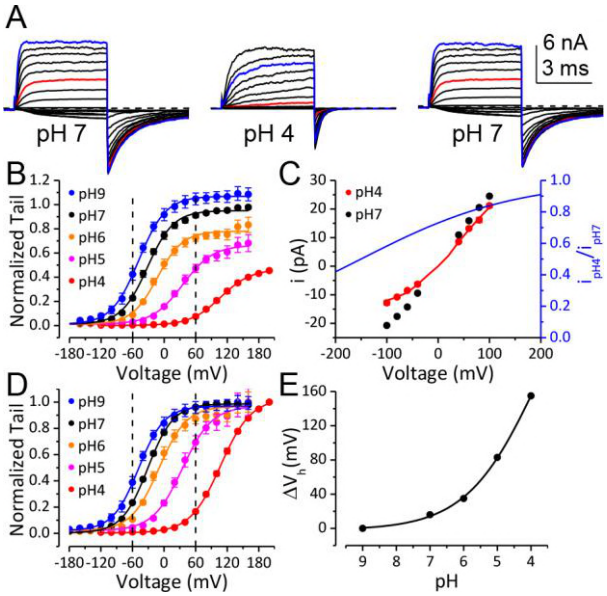

Figure 1. **BK channel activation is strongly inhibited when pH_O is lower than 5.** (A) Macroscopic BK currents recorded from an outside-out patch perfused with extracellular solutions at pH 7 (left), pH 4 (middle), and back to pH 7. Currents were evoked by steps from -160 to +160 mV at pH_O 7 and by steps from -160 mV to +200 mV at pH_O 4 (20 mV increments). The pre- and post-test pulse voltages were -140 and -120 mV, respectively. 300 μM Ca^{2+} was included in pipette (intracellular) solution. The red traces were evoked by +60 mV pulses to highlight the much larger fractional reduction in outward current at this voltage compared to that at +160 mV (blue traces). (B) G-V curves of BK channel generated from tail currents recorded at various pH_Os with values normalized to the maximum value at pH_O 7. Physiologically relevant voltage range (± 60 mV) is marked by two vertical dotted lines. Boltzmann fit results (solid lines) are G_{max} = 1.1 ± 0.01, z = 1 ± 0.03 e, Vh = -49 ± 1.0 mV (pH 9), G_{max} = 1.0 ± 0.01, z = 1 ± 0.04 e, Vh = -32 ± 1.2 mV (pH 7), G_{max} = 0.8 ± 0.01, z = 1 ± 0.05 e, Vh = -13 ± 1.4 mV (pH 6), G_{max} = 0.7 ± 0.01, z = 0.9 ± 0.05 e, Vh = +35 ± 2.3 mV (pH 5), G_{max} = 0.5 ± 0.02, z = 0.9 ± 0.09 e, Vh = +107 ± 3.7 mV (pH 4). (C) Voltage-dependent change of BK single channel current induced by extracellular acidification. The filled dots are the amplitude of BK unitary current at pH_O 7 (black) and 4 (red) measured in the voltage range of ±100 mV. The red line is the prediction of BK unitary current at pH_O 4 by the Woodhull model (refer to materials and methods) with parameters: k_{d0} = 0.27± 0.02 mM (pH 3.6) and δ = 0.17 ±0.02. The blue line is ratio of i_{pH4}/i_{pH7} vs. voltage relationship in the range of ±200 mV as predicted by the Woodhull model. Note that the residual single channel current at -120 mV at pH 4.0 is predicted to be 0.55 of that at pH 7.0, which is comparable to the G_{max} at pH_O 4 in panel B. (D) BK G-V curves as those shown in panel B, but with the values at each pH_O normalized to the maximum value within that pH_O. Physiologically relevant voltage range (± 60 mV) is marked by two vertical dotted lines. Boltzmann fit results (solid lines) are z = 1 ± 0.04 e, V_h = -49 ± 1.2 mV (pH 9), z = 1 ± 0.05 e, V_h = -31 ± 1.1 mV (pH 7), z = 1 ± 0.05 e, V_h = -13 ± 1.2 mV (pH 6), z = 0.9 ± 0.04 e, V_h = +35 ± 1.6 mV (pH 5), z = 0.9 ± 0.06 e, V_h = +107 ± 3.0 mV (pH 4). The V_h and z values are virtually identical to those determined from the G-Vs in Figure 1B. (E) Dose-response curve of BK gating shift (ΔV_h) induced by extracellular H^+. Hill equation ($\Delta V_h = \Delta V_{max}/(1+(IC_{50}/[H^+])^n)$) fit result (solid line) is: IC_{50} = 0.17 ± 0.2 mM (pH 3.8), n = 0.41 ± 0.07.

bioRxiv preprint doi: https://doi.org/10.1101/317339; this version posted May 8, 2018. The copyright holder for this preprint (which was not certified by peer review) is the author/funder, who has granted bioRxiv a license to display the preprint in perpetuity. It is made available under aCC-BY 4.0 International license.

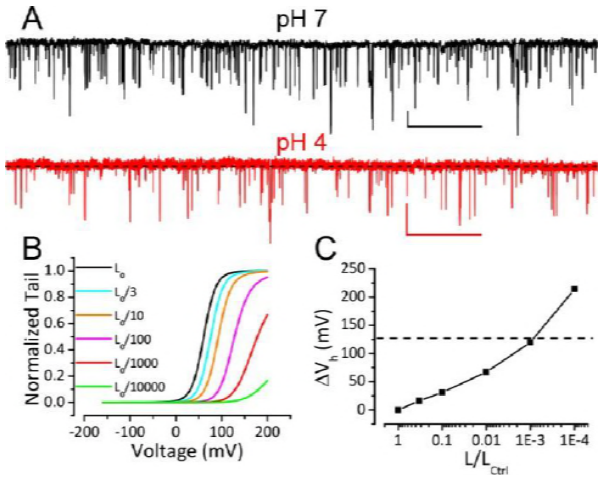

Figure 2. **Reduction of BK C-O equilibrium constant *L* only accounts for a small portion of observed gating shift by extracellular acidification.** (A) BK single channel activity recorded from an outside-out patch hold at -100 mV perfusing in solutions at pH 7 or pH 4. 10 μM Ca^{2+} was included in pipette solution. Opening is downward. The nP_O of the trace at pH 7 is 0.067. The nP_O of the trace at pH 4 is 0.03. Scale bars: 10 pA vertical, 50 ms horizontal. (B) G-V curves calculated using the H-A model with published parameters (Horrigan & Aldrich, 2002) to highlight potential impact of changes in L_0. The zero voltage C-O equilibrium constant L_0 is scaled down from the published value of 10^{-6} (black line, L_{0ctrl}) to shift G-V toward positive potentials. V_h is shifted by +16 mV when L_0 is reduced by 2-fold (cyan line, $L_{0ctrl}/3$). (C) Change of V_h plotted against fold-reduction in L_0. Dotted line marks the change of V_h observed in our experiment when pH_O was changed from 7 to 4.

bioRxiv preprint doi: https://doi.org/10.1101/317339; this version posted May 8, 2018. The copyright holder for this preprint (which was not certified by peer review) is the author/funder, who has granted bioRxiv a license to display the preprint in perpetuity. It is made available under aCC-BY 4.0 International license.

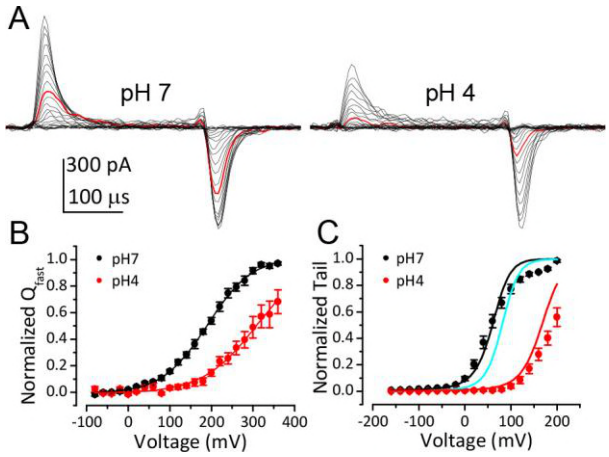

Figure 3. **Inhibition of BK VSD activation is the primary mechanism for BK gating shifts induced by extracellular H^+.** (A) BK gating currents recorded from a macropatch perfused with extracellular solutions at pH 7 (left) or 4 (right). Test pulses were from -80 to +360 mV in 20-mV increments. Red traces were evoked by 200 mV test pulses. (B) Normalized Q_C-V relationship of BK at pH_O 7 and 4. Gray lines are Boltzmann fits (pH7: z_j = 0.46 ± 0.02 *e*, V_{hC} = 190 ± 2.8 mV, pH4: z_j = 0.38 ± 0.02 *e*, V_{hC} = 309 ± 3.0 mV) (C) BK G-V relationships at pH_O 7 or 4 with 10 µM $[Ca^{2+}]_{in}$. The G-V at pH 7 is fit with H-A model using published parameters (Horrigan & Aldrich, 2002) as initial values. z_j and V_{hC} are fixed at the values determined from the Q_C-V relationship at pH 7. The fit results are: K_d = 3 µM, C = 11, D = 24, E = 1, $L_0 = 2.7\times10^{-6}$, z_l = 0.1e (black line). The cyan line is a G-V curve calculated using H-A model with this same set of parameters except that L_0 is reduced by 2-fold (0.9×10^{-6}). The red line is a G-V calculated using the H-A model with V_{hC} and z_j from the Boltzmann fit of Q_C-V at pH 4 and 2-fold reduction in L_0 (0.9×10^{-6}).

bioRxiv preprint doi: https://doi.org/10.1101/317339; this version posted May 8, 2018. The copyright holder for this preprint (which was not certified by peer review) is the author/funder, who has granted bioRxiv a license to display the preprint in perpetuity. It is made available under aCC-BY 4.0 International license.

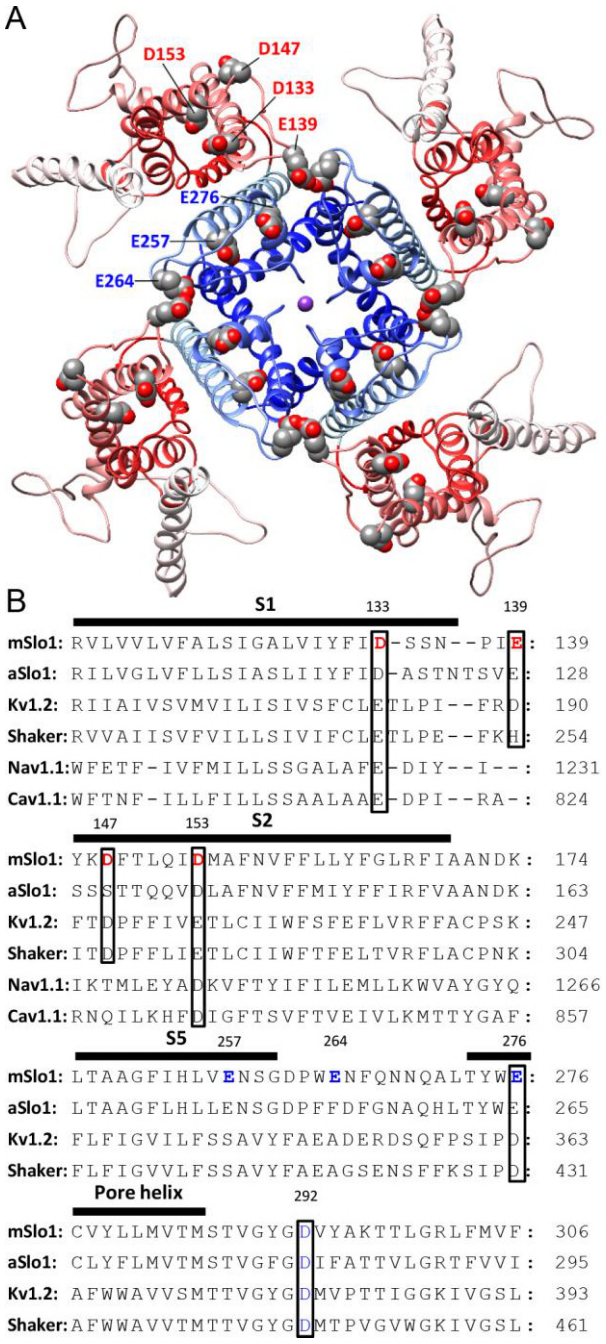

Figure 4. **BK acidic residues potentially exposed to extracellular medium.** (A) mSlo1 homology model based on the cryo-EM structure of liganded Aplysia BK channel (PDB: 5tj6) viewed from the extracellular side. Acidic residues potentially exposed to extracellular solution are rendered as spheres with oxygen and carbon colored in red and gray, respectively. The BK VSDs and PGD are colored in red and blue, respectively. The purple dot in the center is K^+. (B) Multiple sequence alignment of transmembrane segments containing extracellularly accessible acidic residues from mouse and Aplysia homologues of Slo1 (mSlo1, aSlo1), Kv channels (Kv1.2, *Shaker*), and human Nav1.1 and Cav1.1 channels. For the latter two channels, only the DIII VSD segments were included in the alignment. Extracellularly accessible acidic residues conserved among these channels are indicated by boxes. Residues examined in the present study are bold.

bioRxiv preprint doi: https://doi.org/10.1101/317339; this version posted May 8, 2018. The copyright holder for this preprint (which was not certified by peer review) is the author/funder, who has granted bioRxiv a license to display the preprint in perpetuity. It is made available under aCC-BY 4.0 International license.

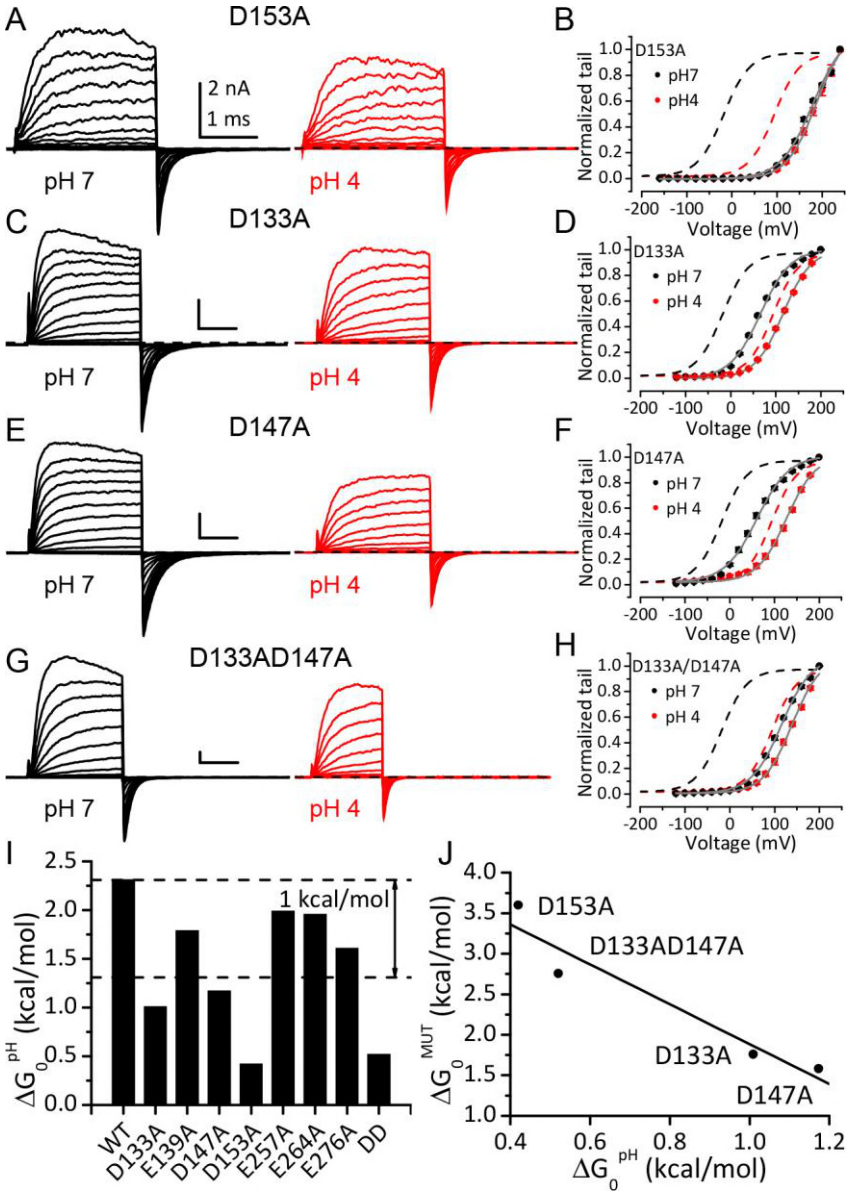

Figure 5. **Acidic residues involved in BK inhibition induced by extracellular H^+**. (A) Macroscopic currents of mSlo1D153A from an outside-out patch perfused at pH_O 7 (left) or pH_O 4 (right). The currents of D153A were evoked by steps from -160 to +240 mV with 20 mV increments. All other currents shown in this figure were evoked by steps from -120 to +200 mV (20 mV increments). All pipette (intracellular) solutions contained 300 μM Ca^{2+}. (B) The G-V curves of D153A at pH_O 7 or 4. Boltzmann fit results (grey lines) are z = 0.7 ± 0.03e, V_h = 179 ± 2.4 mV (pH 7), z = 0.8 ± 0.03e, V_h = 186 ± 2.2 mV (pH 4), G_{max} = 1.16± 0.03. Dotted lines in this and following G-V plots are the G-V curves of WT channels at pH7 (black) or 4 (red) with 300 μM $[Ca^{2+}]_{in}$ (C) Macroscopic currents of mSlo1D133A at pH_O 7 (left) or pH 4 (right). (D) The G-V curves of D133A at pH_O 7 or 4. Boltzmann fit results (grey lines) are z = 0.8 ± 0.03e, V_h = 66 ± 1.7 mV (pH 7), z = 0.8 ± 0.03e, V_h = 116 ± 1.6 mV (pH 4), G_{max} = 1.00± 0.02. (E) Macroscopic currents of mSlo1D147A at pH_O 7 (left) or pH 4 (right). (F) The G-V curves of D147A at pH_O 7 or 4. Boltzmann fit results (grey lines) are z = 0.7 ± 0.04 e, V_h = 61 ± 2.6 mV (pH 7), z = 0.8 ± 0.05e, V_h = 127 ± 2.3 mV (pH 4), G_{max} = 1.00± 0.02. (G) Macroscopic currents of mSlo1D133A147A at pH_O 7 (left) or pH 4 (right). (H) The G-V curves of mSlo1D133AD147A at pH_O 7 or 4. Boltzmann fit results (grey lines) are z = 0.7 ± 0.04e, V_h = 116 ± 2.3 mV (pH 7), z = 0.8 ± 0.04e, V_h = 139± 2.1 mV (pH 4), G_{max} = 1.07± 0.03. (I) Change of gating equilibrium free

bioRxiv preprint doi: https://doi.org/10.1101/317339; this version posted May 8, 2018. The copyright holder for this preprint (which was not certified by peer review) is the author/funder, who has granted bioRxiv a license to display the preprint in perpetuity. It is made available under aCC-BY 4.0 International license.

energy by extracellular acidification(ΔG_0^{pH}) calculated from the Boltzmann fits of G-V curves. (J) The change of gating equilibrium free energy by alanine substitution (ΔG_0^{MUT}) plotted against the change of gating equilibrium free energy by extracellular acidification (ΔG_0^{pH}). The solid line is a linear fit with R of 0.96.

bioRxiv preprint doi: https://doi.org/10.1101/317339; this version posted May 8, 2018. The copyright holder for this preprint (which was not certified by peer review) is the author/funder, who has granted bioRxiv a license to display the preprint in perpetuity. It is made available under aCC-BY 4.0 International license.

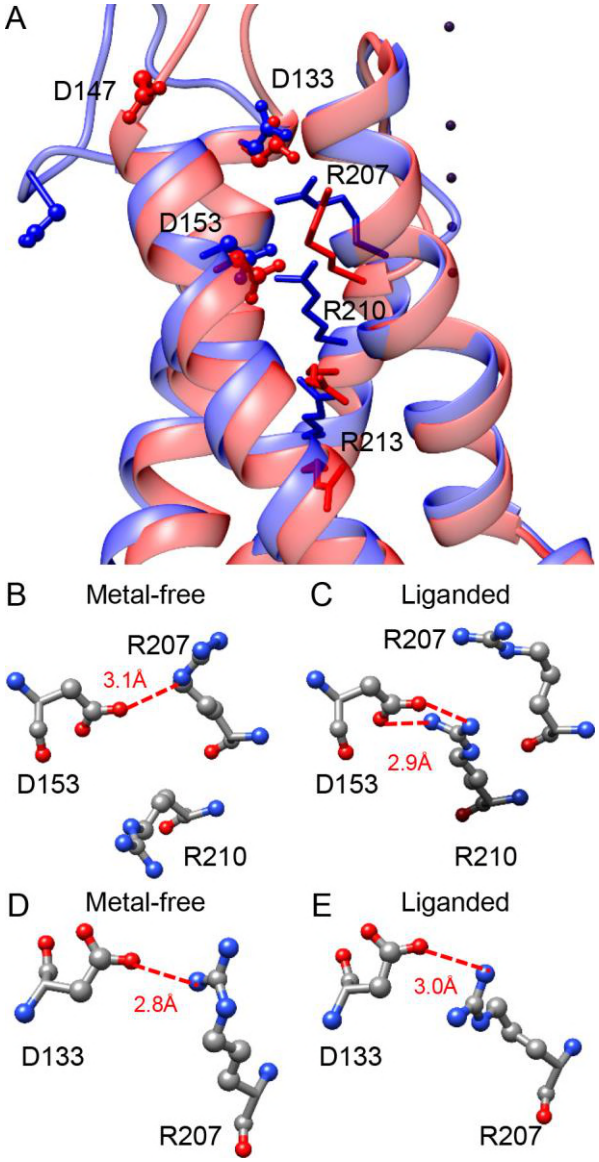

Figure 6. (A) The VSDs of metal-free (red) and liganded (blue) mSlo1 structures with three key acidic residues rendered as ball-and-chain and three conserved S4 arginines (homologous to Shaker R2, R3 and R4) rendered as sticks. The four dark purple dots are K^+s in the BK selectivity filter, which are included as a reference for vertical displacement. The two structures are superimposed by the pore-loop. (B) D153 may form a hydrogen bond with R207 in the metal-free mSlo1 structure. The distance between the side chains of D153 and R210 is more than 6 Å, which is too far for hydrogen bonding. (C) D153 may form a hydrogen bond with R210 in the liganded mSlo1 structure. The distance between the side chains of D153 and R207 is more than 4 Å, which is also beyond the limit of effective hydrogen bonding. (D-E) The distances between the side chains of D133 and R207 in both the metal-free (D) and the liganded (E) structures are within 3 Å, allowing potential interaction between D133 and R207 in both conformations.

bioRxiv preprint doi: https://doi.org/10.1101/317339; this version posted May 8, 2018. The copyright holder for this preprint (which was not certified by peer review) is the author/funder, who has granted bioRxiv a license to display the preprint in perpetuity. It is made available under aCC-BY 4.0 International license.

Acknowledgements: This work was supported by NIH grant GM118114 to CJL.

Competing interests: We have no conflicts of interest to disclose.

bioRxiv preprint doi: https://doi.org/10.1101/317339; this version posted May 8, 2018. The copyright holder for this preprint (which was not certified by peer review) is the author/funder, who has granted bioRxiv a license to display the preprint in perpetuity. It is made available under aCC-BY 4.0 International license.

Reference List

Armstrong, C. M. & Bezanilla, F. (1974). Charge movement associated with the opening and closing of the activation gates of the Na channels. *J.Gen.Physiol, 63,* 533-552.

Avdonin, V., Tang, X. D., & Hoshi, T. (2003). Stimulatory action of internal protons on Slo1 BK channels. *Biophys.J., 84,* 2969-2980.

Bailey, M. A., Cantone, A., Yan, Q., MacGregor, G. G., Leng, Q., Amorim, J. B. et al. (2006). Maxi-K channels contribute to urinary potassium excretion in the ROMK-deficient mouse model of Type II Bartter's syndrome and in adaptation to a high-K diet. *Kidney Int., 70,* 51-59.

Brenner, R., Chen, Q. H., Vilaythong, A., Toney, G. M., Noebels, J. L., & Aldrich, R. W. (2005). BK channel beta4 subunit reduces dentate gyrus excitability and protects against temporal lobe seizures. *Nat.Neurosci., 8,* 1752-1759.

Brenner, R., Perez, G. J., Bonev, A. D., Eckman, D. M., Kosek, J. C., Wiler, S. W. et al. (2000). Vasoregulation by the beta1 subunit of the calcium-activated potassium channel. *Nature, 407,* 870-876.

Bright, N. A., Davis, L. J., & Luzio, J. P. (2016). Endolysosomes Are the Principal Intracellular Sites of Acid Hydrolase Activity. *Curr.Biol., 26,* 2233-2245.

Cao, Q., Zhong, X. Z., Zou, Y., Zhang, Z., Toro, L., & Dong, X. P. (2015). BK Channels Alleviate Lysosomal Storage Diseases by Providing Positive Feedback Regulation of Lysosomal Ca^{2+} Release. *Dev.Cell, 33,* 427-441.

Christensen, O. & Zeuthen, T. (1987). Maxi K+ channels in leaky epithelia are regulated by intracellular Ca2+, pH and membrane potential. *Pflugers Arch., 408,* 249-259.

bioRxiv preprint doi: https://doi.org/10.1101/317339; this version posted May 8, 2018. The copyright holder for this preprint (which was not certified by peer review) is the author/funder, who has granted bioRxiv a license to display the preprint in perpetuity. It is made available under aCC-BY 4.0 International license.

Claydon, T. W., Boyett, M. R., Sivaprasadarao, A., Ishii, K., Owen, J. M., O'Beirne, H. A. et al. (2000). Inhibition of the K^+ channel kv1.4 by acidosis: protonation of an extracellular histidine slows the recovery from N-type inactivation. *J.Physiol, 526 Pt 2,* 253-264.

Claydon, T. W., Kehl, S. J., & Fedida, D. (2008). Closed-state inactivation induced in K(V)1 channels by extracellular acidification. *Channels (Austin.), 2,* 139-142.

Claydon, T. W., Vaid, M., Rezazadeh, S., Kwan, D. C., Kehl, S. J., & Fedida, D. (2007). A direct demonstration of closed-state inactivation of K^+ channels at low pH. *J.Gen.Physiol, 129,* 437-455.

Cook, D. L., Ikeuchi, M., & Fujimoto, W. Y. (1984). Lowering of pHi inhibits Ca2+-activated K+ channels in pancreatic B-cells. *Nature, 311,* 269-271.

Deutsch, C. & Lee, S. C. (1989). Modulation of K^+ currents in human lymphocytes by pH. *J.Physiol, 413,* 399-413.

DiChiara, T. J. & Reinhart, P. H. (1995). Distinct effects of Ca2+ and voltage on the activation and deactivation of cloned Ca(2+)-activated K+ channels. *J.Physiol, 489 (Pt 2),* 403-418.

Grimm, P. R., Foutz, R. M., Brenner, R., & Sansom, S. C. (2007). Identification and localization of BK-beta subunits in the distal nephron of the mouse kidney. *Am.J.Physiol Renal Physiol, 293,* F350-F359.

Guarina, L., Vandael, D. H., Carabelli, V., & Carbone, E. (2017). Low pHo boosts burst firing and catecholamine release by blocking TASK-1 and BK channels while preserving Cav1 channels in mouse chromaffin cells. *J.Physiol, 595,* 2587-2609.

Hamill, O. P., Marty, A., Neher, E., Sakmann, B., & Sigworth, F. J. (1981). Improved patch-clamp techniques for high-resolution current recording from cells and cell-free membrane patches. *Pflugers Arch., 391,* 85-100.

bioRxiv preprint doi: https://doi.org/10.1101/317339; this version posted May 8, 2018. The copyright holder for this preprint (which was not certified by peer review) is the author/funder, who has granted bioRxiv a license to display the preprint in perpetuity. It is made available under aCC-BY 4.0 International license.

Haug, T., Olcese, R., Toro, L., & Stefani, E. (2004). Regulation of K^+ flow by a ring of negative charges in the outer pore of BKCa channels. Part II: Neutralization of aspartate 292 reduces long channel openings and gating current slow component. *J.Gen.Physiol, 124,* 185-197.

Haug, T., Sigg, D., Ciani, S., Toro, L., Stefani, E., & Olcese, R. (2004). Regulation of K^+ flow by a ring of negative charges in the outer pore of BKCa channels. Part I: Aspartate 292 modulates K^+ conduction by external surface charge effect. *J.Gen.Physiol, 124,* 173-184.

Heitzmann, D. & Warth, R. (2007). No potassium, no acid: K^+ channels and gastric acid secretion. *Physiology.(Bethesda.), 22,* 335-341.

Hite, R. K., Tao, X., & MacKinnon, R. (2017). Structural basis for gating the high-conductance Ca^{2+}-activated K^+ channel. *Nature, 541,* 52-57.

Horrigan, F. T. & Aldrich, R. W. (1999). Allosteric voltage gating of potassium channels II. Mslo channel gating charge movement in the absence of Ca(2+). *J.Gen.Physiol, 114,* 305-336.

Horrigan, F. T. & Aldrich, R. W. (2002). Coupling between voltage sensor activation, Ca^{2+} binding and channel opening in large conductance (BK) potassium channels. *J.Gen.Physiol, 120,* 267-305.

Horrigan, F. T., Cui, J., & Aldrich, R. W. (1999). Allosteric voltage gating of potassium channels I. Mslo ionic currents in the absence of Ca(2+). *J.Gen.Physiol, 114,* 277-304.

Horrigan, F. T., Heinemann, S. H., & Hoshi, T. (2005). Heme regulates allosteric activation of the Slo1 BK channel. *J.Gen.Physiol, 126,* 7-21.

Horrigan, F. T. & Ma, Z. (2008). Mg^{2+} enhances voltage sensor/gate coupling in BK channels. *J.Gen.Physiol, 131,* 13-32.

bioRxiv preprint doi: https://doi.org/10.1101/317339; this version posted May 8, 2018. The copyright holder for this preprint (which was not certified by peer review) is the author/funder, who has granted bioRxiv a license to display the preprint in perpetuity. It is made available under aCC-BY 4.0 International license.

Hoshi, T., Tian, Y., Xu, R., Heinemann, S. H., & Hou, S. (2013). Mechanism of the modulation of BK potassium channel complexes with different auxiliary subunit compositions by the omega-3 fatty acid DHA. *Proc.Natl.Acad.Sci.U.S.A, 110,* 4822-4827.

Hoshi, T., Wissuwa, B., Tian, Y., Tajima, N., Xu, R., Bauer, M. et al. (2013). Omega-3 fatty acids lower blood pressure by directly activating large-conductance Ca(2)(+)-dependent K(+) channels. *Proc.Natl.Acad.Sci.U.S.A, 110,* 4816-4821.

Hou, S., Heinemann, S. H., & Hoshi, T. (2009). Modulation of BKCa channel gating by endogenous signaling molecules. *Physiology.(Bethesda.), 24,* 26-35.

Hou, S., Xu, R., Heinemann, S. H., & Hoshi, T. (2008a). Reciprocal regulation of the Ca2+ and H+ sensitivity in the SLO1 BK channel conferred by the RCK1 domain. *Nat.Struct.Mol.Biol., 15,* 403-410.

Hou, S., Xu, R., Heinemann, S. H., & Hoshi, T. (2008b). The RCK1 high-affinity Ca2+ sensor confers carbon monoxide sensitivity to Slo1 BK channels. *Proc.Natl.Acad.Sci.U.S.A, 105,* 4039-4043.

Jiang, Y., Pico, A., Cadene, M., Chait, B. T., & MacKinnon, R. (2001). Structure of the RCK domain from the E. coli K^+ channel and demonstration of its presence in the human BK channel. *Neuron, 29,* 593-601.

Johnson, D. E., Ostrowski, P., Jaumouille, V., & Grinstein, S. (2016). The position of lysosomes within the cell determines their luminal pH. *J.Cell Biol., 212,* 677-692.

Kwan, D. C., Fedida, D., & Kehl, S. J. (2006). Single channel analysis reveals different modes of Kv1.5 gating behavior regulated by changes of external pH. *Biophys.J., 90,* 1212-1222.

Latorre, R., Vergara, C., & Hidalgo, C. (1982). Reconstitution in planar lipid bilayers of a Ca2+-dependent K+ channel from transverse tubule membranes isolated from rabbit skeletal muscle. *Proc.Natl.Acad.Sci.U.S.A, 79,* 805-809.

bioRxiv preprint doi: https://doi.org/10.1101/317339; this version posted May 8, 2018. The copyright holder for this preprint (which was not certified by peer review) is the author/funder, who has granted bioRxiv a license to display the preprint in perpetuity. It is made available under aCC-BY 4.0 International license.

Li, B., Jie, W., Huang, L., Wei, P., Li, S., Luo, Z. et al. (2014). Nuclear BK channels regulate gene expression via the control of nuclear calcium signaling. *Nat.Neurosci., 17,* 1055-1063.

Ma, Z., Lou, X. J., & Horrigan, F. T. (2006). Role of charged residues in the S1-S4 voltage sensor of BK channels. *J.Gen.Physiol, 127,* 309-328.

Ma, Z., Wong, K. Y., & Horrigan, F. T. (2008). An extracellular Cu^{2+} binding site in the voltage sensor of BK and Shaker potassium channels. *J.Gen.Physiol, 131,* 483-502.

Magleby, K. L. & Pallotta, B. S. (1983). Calcium dependence of open and shut interval distributions from calcium-activated potassium channels in cultured rat muscle. *J.Physiol, 344,* 585-604.

Meredith, A. L., Wiler, S. W., Miller, B. H., Takahashi, J. S., Fodor, A. A., Ruby, N. F. et al. (2006). BK calcium-activated potassium channels regulate circadian behavioral rhythms and pacemaker output. *Nat.Neurosci., 9,* 1041-1049.

Mindell, J. A. (2012). Lysosomal acidification mechanisms. *Annu.Rev.Physiol, 74,* 69-86.

Pettersen, E. F., Goddard, T. D., Huang, C. C., Couch, G. S., Greenblatt, D. M., Meng, E. C. et al. (2004). UCSF Chimera--a visualization system for exploratory research and analysis. *J.Comput.Chem., 25,* 1605-1612.

Prole, D. L., Lima, P. A., & Marrion, N. V. (2003). Mechanisms underlying modulation of neuronal KCNQ2/KCNQ3 potassium channels by extracellular protons. *J.Gen.Physiol, 122,* 775-793.

Reinhart, P. H., Chung, S., Martin, B. L., Brautigan, D. L., & Levitan, I. B. (1991). Modulation of calcium-activated potassium channels from rat brain by protein kinase A and phosphatase 2A. *J.Neurosci., 11,* 1627-1635.

bioRxiv preprint doi: https://doi.org/10.1101/317339; this version posted May 8, 2018. The copyright holder for this preprint (which was not certified by peer review) is the author/funder, who has granted bioRxiv a license to display the preprint in perpetuity. It is made available under aCC-BY 4.0 International license.

Robitaille, R., Garcia, M. L., Kaczorowski, G. J., & Charlton, M. P. (1993). Functional colocalization of calcium and calcium-gated potassium channels in control of transmitter release. *Neuron, 11,* 645-655.

Rosenblatt, K. P., Sun, Z. P., Heller, S., & Hudspeth, A. J. (1997). Distribution of Ca^{2+}-activated K^+ channel isoforms along the tonotopic gradient of the chicken's cochlea. *Neuron, 19,* 1061-1075.

Sali, A. & Blundell, T. L. (1993). Comparative protein modelling by satisfaction of spatial restraints. *J.Mol.Biol., 234,* 779-815.

Schreiber, M. & Salkoff, L. (1997). A novel calcium-sensing domain in the BK channel. *Biophys.J., 73,* 1355-1363.

Schubert, R., Krien, U., & Gagov, H. (2001). Protons inhibit the BK(Ca) channel of rat small artery smooth muscle cells. *J.Vasc.Res., 38,* 30-38.

Shi, J. & Cui, J. (2001). Intracellular Mg^{2+} enhances the function of BK-type Ca(2+)-activated K(+) channels. *J.Gen.Physiol, 118,* 589-606.

Shi, J., Krishnamoorthy, G., Yang, Y., Hu, L., Chaturvedi, N., Harilal, D. et al. (2002). Mechanism of magnesium activation of calcium-activated potassium channels. *Nature, 418,* 876-880.

Singh, H., Lu, R., Bopassa, J. C., Meredith, A. L., Stefani, E., & Toro, L. (2013). MitoBK(Ca) is encoded by the Kcnma1 gene, and a splicing sequence defines its mitochondrial location. *Proc.Natl.Acad.Sci.U.S.A, 110,* 10836-10841.

Tanaka, Y., Koike, K., Alioua, A., Shigenobu, K., Stefani, E., & Toro, L. (2004). Beta1-subunit of MaxiK channel in smooth muscle: a key molecule which tunes muscle mechanical activity. *J.Pharmacol.Sci., 94,* 339-347.

bioRxiv preprint doi: https://doi.org/10.1101/317339; this version posted May 8, 2018. The copyright holder for this preprint (which was not certified by peer review) is the author/funder, who has granted bioRxiv a license to display the preprint in perpetuity. It is made available under aCC-BY 4.0 International license.

Tang, X. D., Xu, R., Reynolds, M. F., Garcia, M. L., Heinemann, S. H., & Hoshi, T. (2003). Haem can bind to and inhibit mammalian calcium-dependent Slo1 BK channels. *Nature, 425,* 531-535.

Tao, X., Hite, R. K., & MacKinnon, R. (2017). Cryo-EM structure of the open high-conductance Ca^{2+}-activated K^+ channel. *Nature, 541,* 46-51.

Tian, L., Coghill, L. S., McClafferty, H., MacDonald, S. H., Antoni, F. A., Ruth, P. et al. (2004). Distinct stoichiometry of BKCa channel tetramer phosphorylation specifies channel activation and inhibition by cAMP-dependent protein kinase. *Proc.Natl.Acad.Sci.U.S.A, 101,* 11897-11902.

Tian, L., McClafferty, H., Chen, L., & Shipston, M. J. (2008). Reversible tyrosine protein phosphorylation regulates large conductance voltage- and calcium-activated potassium channels via cortactin. *J.Biol.Chem., 283,* 3067-3076.

Tiwari-Woodruff, S. K., Lin, M. A., Schulteis, C. T., & Papazian, D. M. (2000). Voltage-dependent structural interactions in the Shaker K(+) channel. *J.Gen.Physiol, 115,* 123-138.

Tseng-Crank, J., Foster, C. D., Krause, J. D., Mertz, R., Godinot, N., DiChiara, T. J. et al. (1994). Cloning, expression, and distribution of functionally distinct Ca(2+)-activated K+ channel isoforms from human brain. *Neuron, 13,* 1315-1330.

Wagner, C. A., Finberg, K. E., Breton, S., Marshansky, V., Brown, D., & Geibel, J. P. (2004). Renal vacuolar H^+-ATPase. *Physiol Rev., 84,* 1263-1314.

Wallner, M., Meera, P., & Toro, L. (1996). Determinant for beta-subunit regulation in high-conductance voltage-activated and Ca(2+)-sensitive K^+ channels: an additional transmembrane region at the N terminus. *Proc.Natl.Acad.Sci.U.S.A, 93,* 14922-14927.

bioRxiv preprint doi: https://doi.org/10.1101/317339; this version posted May 8, 2018. The copyright holder for this preprint (which was not certified by peer review) is the author/funder, who has granted bioRxiv a license to display the preprint in perpetuity. It is made available under aCC-BY 4.0 International license.

Wang, W., Zhang, X., Gao, Q., Lawas, M., Yu, L., Cheng, X. et al. (2017). A voltage-dependent K+ channel in the lysosome is required for refilling lysosomal Ca2+ stores. *J.Cell Biol., 216,* 1715-1730.

Wellman, G. C. & Nelson, M. T. (2003). Signaling between SR and plasmalemma in smooth muscle: sparks and the activation of Ca^{2+}-sensitive ion channels. *Cell Calcium, 34,* 211-229.

Woodhull, A. M. (1973). Ionic blockage of sodium channels in nerve. *J.Gen.Physiol, 61,* 687-708.

Xia, X. M., Ding, J. P., & Lingle, C. J. (1999). Molecular basis for the inactivation of Ca^{2+}- and voltage-dependent BK channels in adrenal chromaffin cells and rat insulinoma tumor cells. *J.Neurosci., 19,* 5255-5264.

Xia, X. M., Ding, J. P., Zeng, X. H., Duan, K. L., & Lingle, C. J. (2000). Rectification and rapid activation at low Ca^{2+} of Ca^{2+}-activated, voltage-dependent BK currents: consequences of rapid inactivation by a novel beta subunit. *J.Neurosci., 20,* 4890-4903.

Xia, X. M., Zeng, X., & Lingle, C. J. (2002). Multiple regulatory sites in large-conductance calcium-activated potassium channels. *Nature, 418,* 880-884.

Xia, X. M., Zhang, X., & Lingle, C. J. (2004). Ligand-dependent activation of Slo family channels is defined by interchangeable cytosolic domains. *J.Neurosci., 24,* 5585-5591.

Xu, H. & Ren, D. (2015). Lysosomal physiology. *Annu.Rev.Physiol, 77,* 57-80.

Yan, J. & Aldrich, R. W. (2010). LRRC26 auxiliary protein allows BK channel activation at resting voltage without calcium. *Nature, 466,* 513-516.

Yifrach, O. & MacKinnon, R. (2002). Energetics of pore opening in a voltage-gated K(+) channel. *Cell, 111,* 231-239.

bioRxiv preprint doi: https://doi.org/10.1101/317339; this version posted May 8, 2018. The copyright holder for this preprint (which was not certified by peer review) is the author/funder, who has granted bioRxiv a license to display the preprint in perpetuity. It is made available under aCC-BY 4.0 International license.

Zhang, S., Kurata, H. T., Kehl, S. J., & Fedida, D. (2003). Rapid induction of P/C-type inactivation is the mechanism for acid-induced K^+ current inhibition. *J.Gen.Physiol, 121,* 215-225.

Zhang, X., Solaro, C. R., & Lingle, C. J. (2001). Allosteric regulation of BK channel gating by Ca(2+) and Mg(2+) through a nonselective, low affinity divalent cation site. *J.Gen.Physiol, 118,* 607-636.

Zhou, Y. & Lingle, C. J. (2014). Paxilline inhibits BK channels by an almost exclusively closed-channel block mechanism. *J.Gen.Physiol, 144,* 415-440.

Zhou, Y., Tang, Q. Y., Xia, X. M., & Lingle, C. J. (2010). Glycine311, a determinant of paxilline block in BK channels: a novel bend in the BK S6 helix. *J.Gen.Physiol, 135,* 481-494.

bioRxiv preprint doi: https://doi.org/10.1101/317339; this version posted May 8, 2018. The copyright holder for this preprint (which was not certified by peer review) is the author/funder, who has granted bioRxiv a license to display the preprint in perpetuity. It is made available under aCC-BY 4.0 International license.

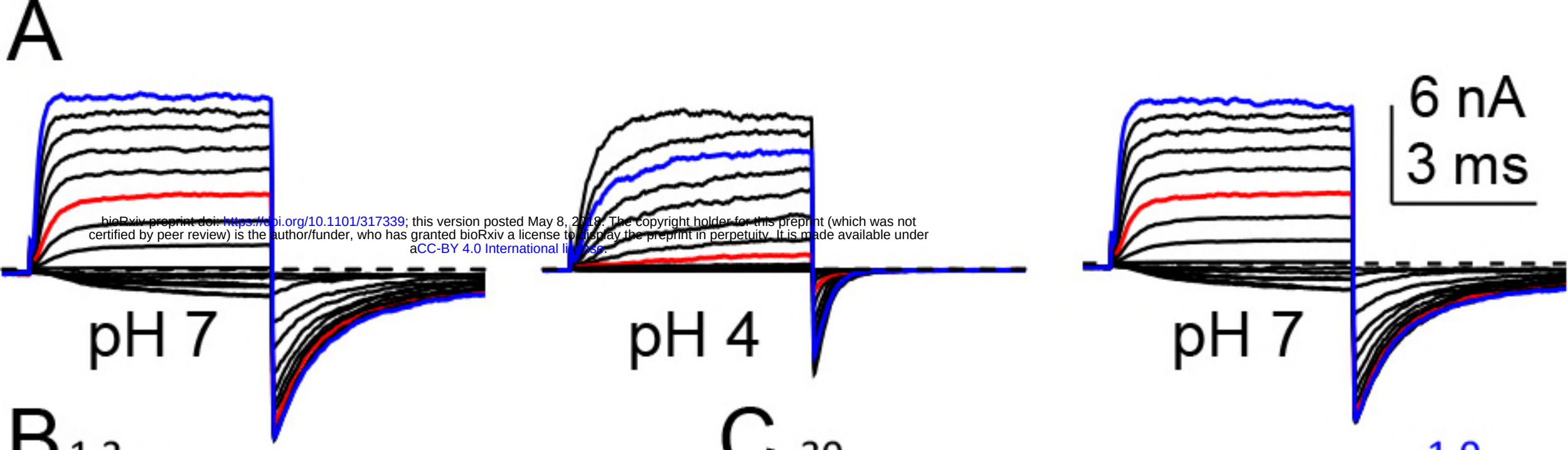

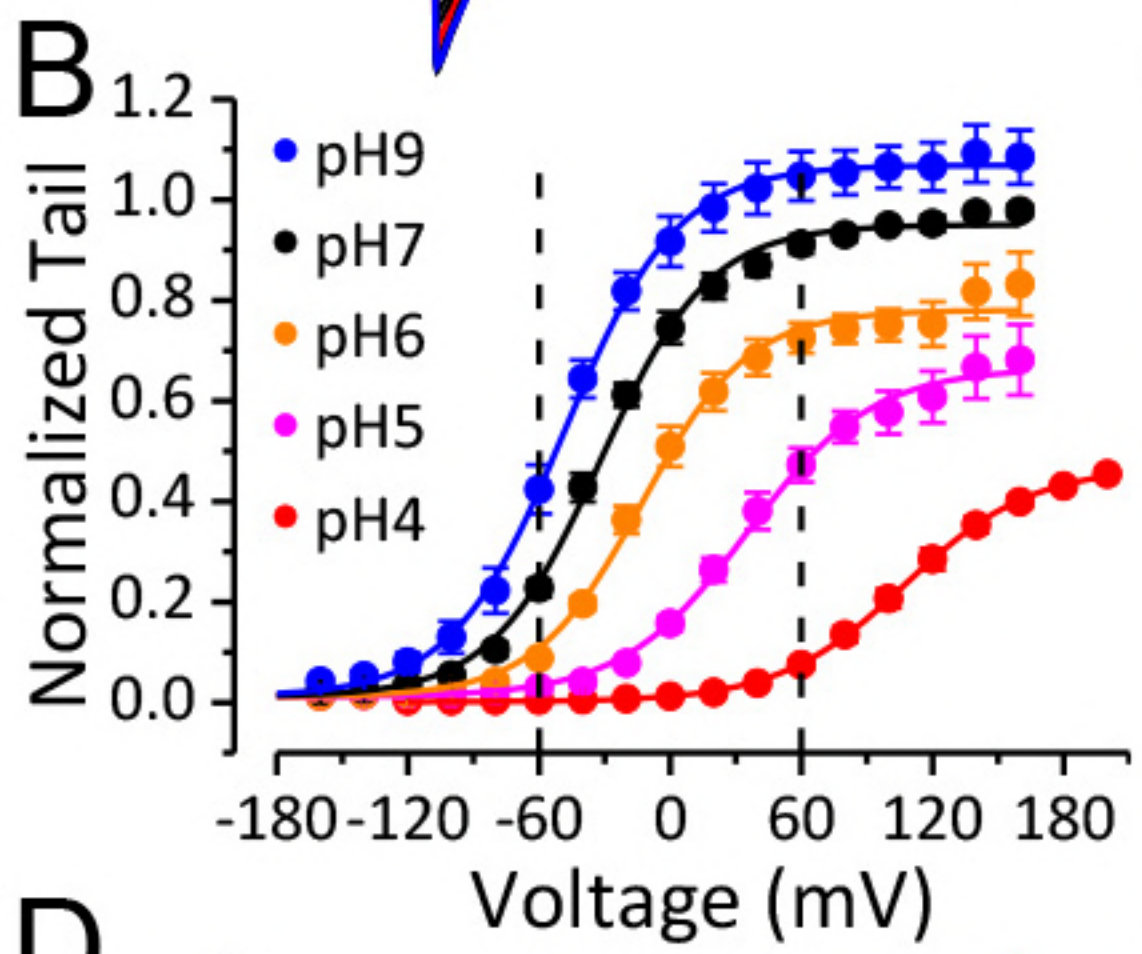

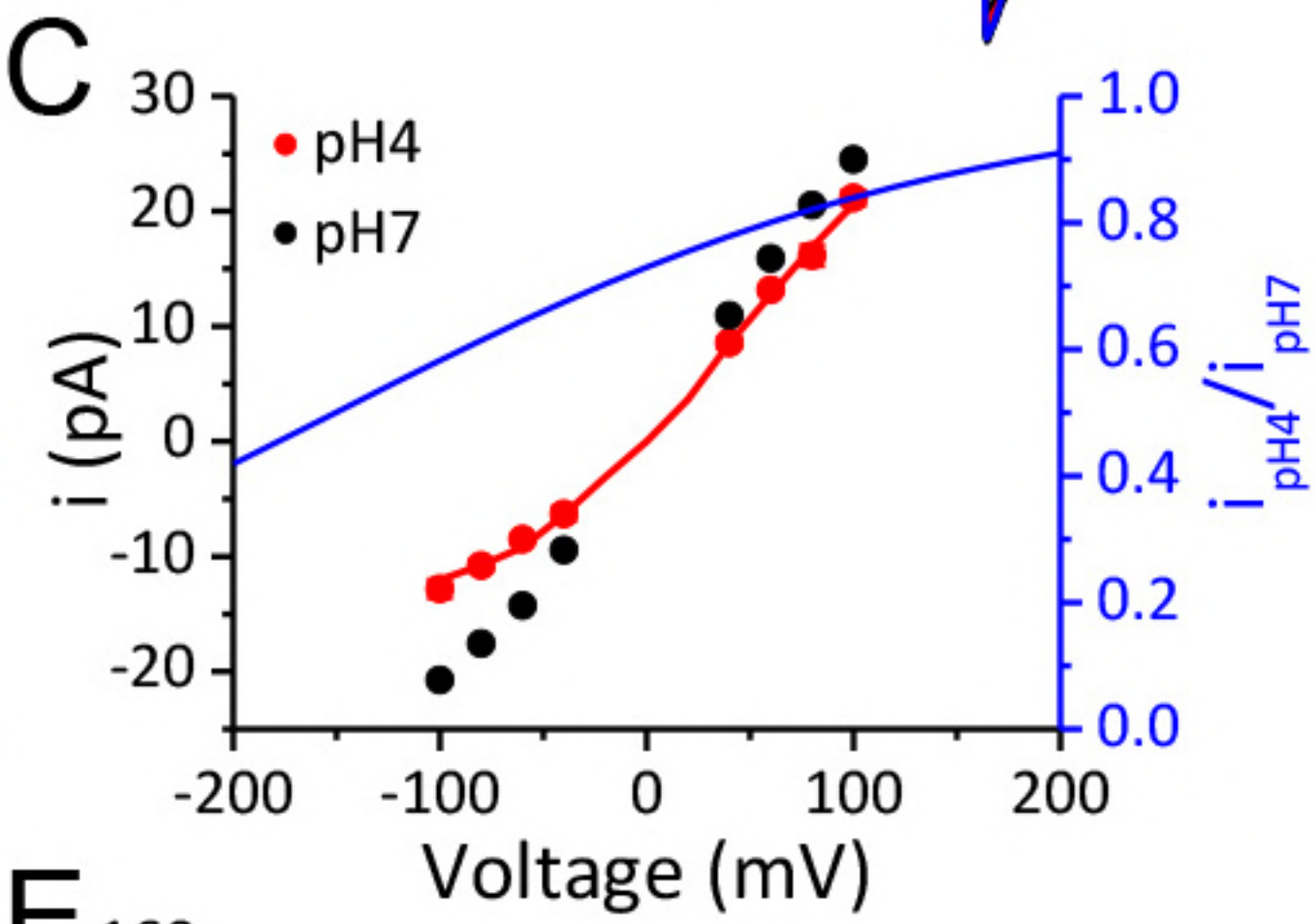

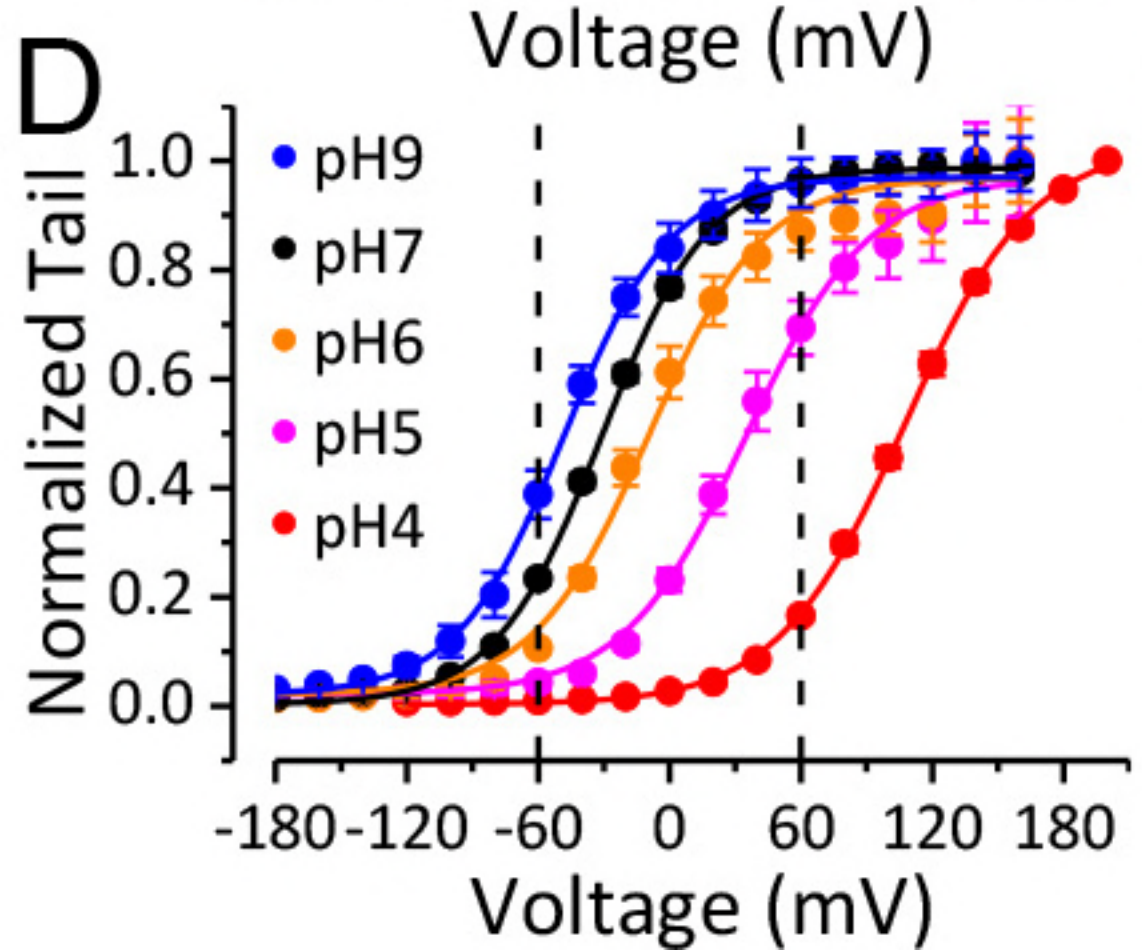

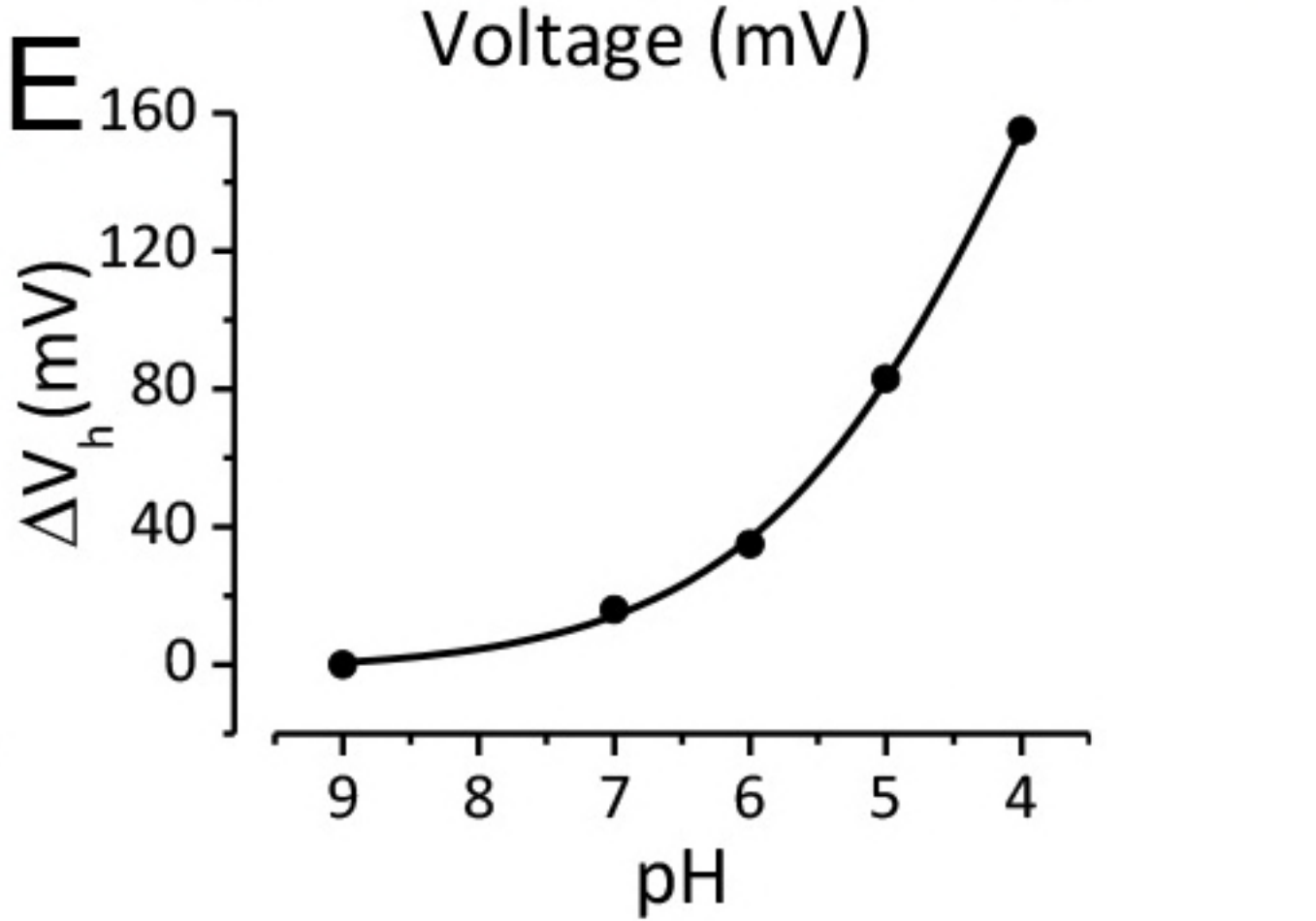

A

pH 7

pH 4

B

Normalized Tail

1.0
0.8
0.6
0.4
0.2
0.0

L_0
$L_0/3$
$L_0/10$
$L_0/100$
$L_0/1000$
$L_0/10000$

-200 -100 0 100 200

Voltage (mV)

C

ΔV_h (mV)

250
200
150
100
50
0

1 0.1 0.01 1E-3 1E-4

L/L_{Ctrl}

A

pH 7

300 pA

100 µs

pH 4

B

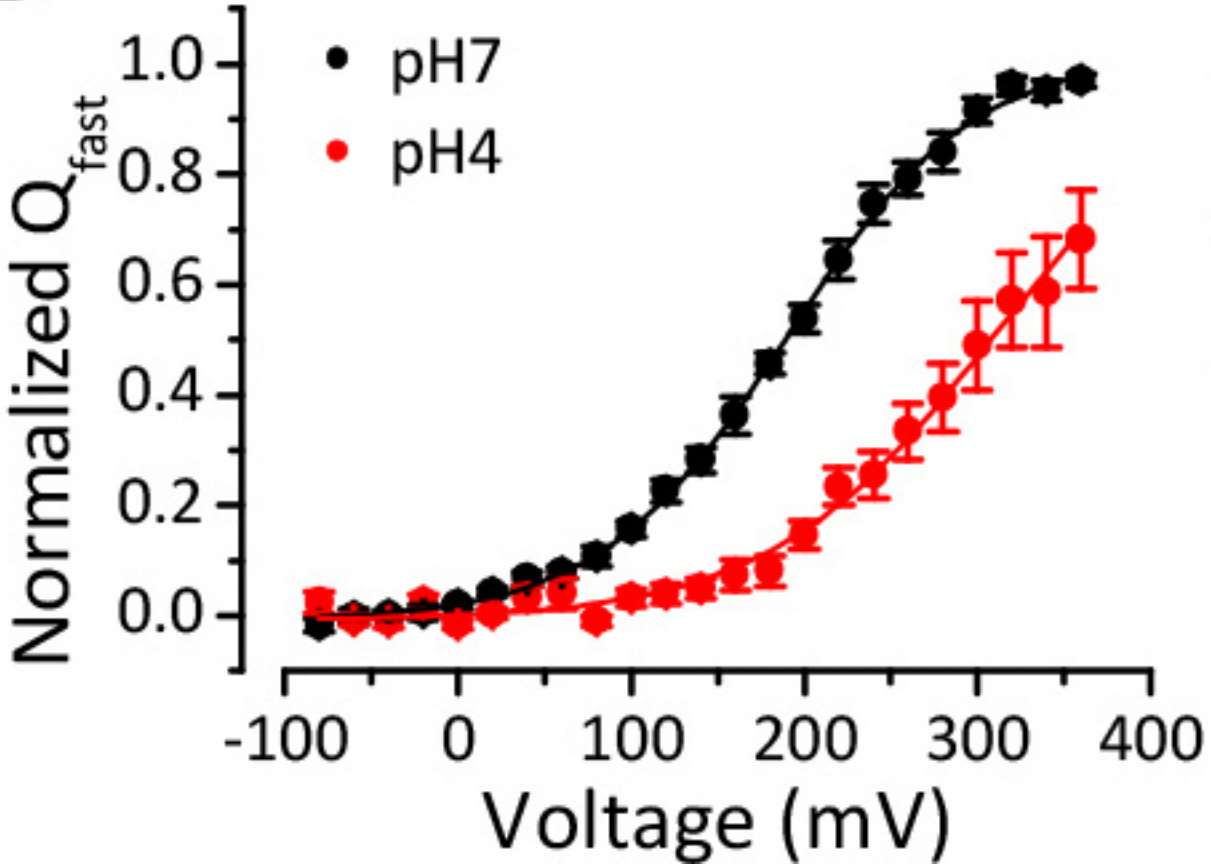

C

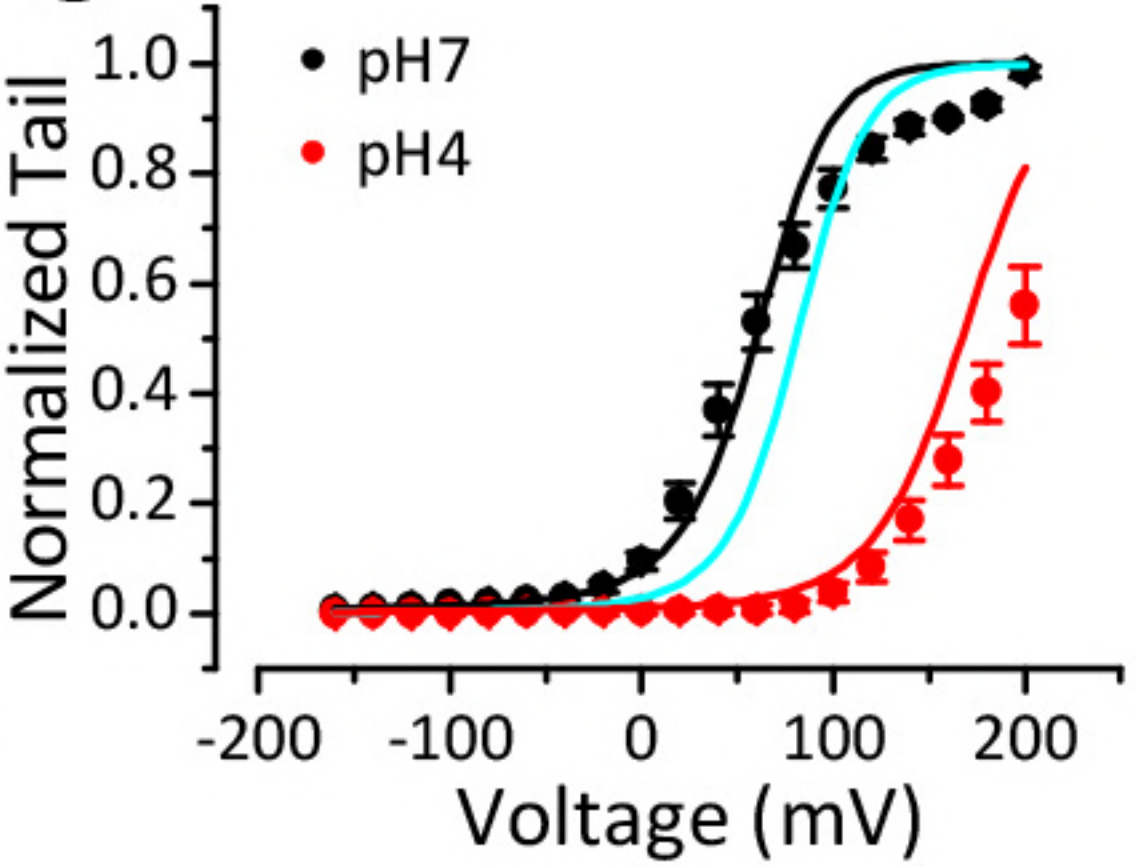

A

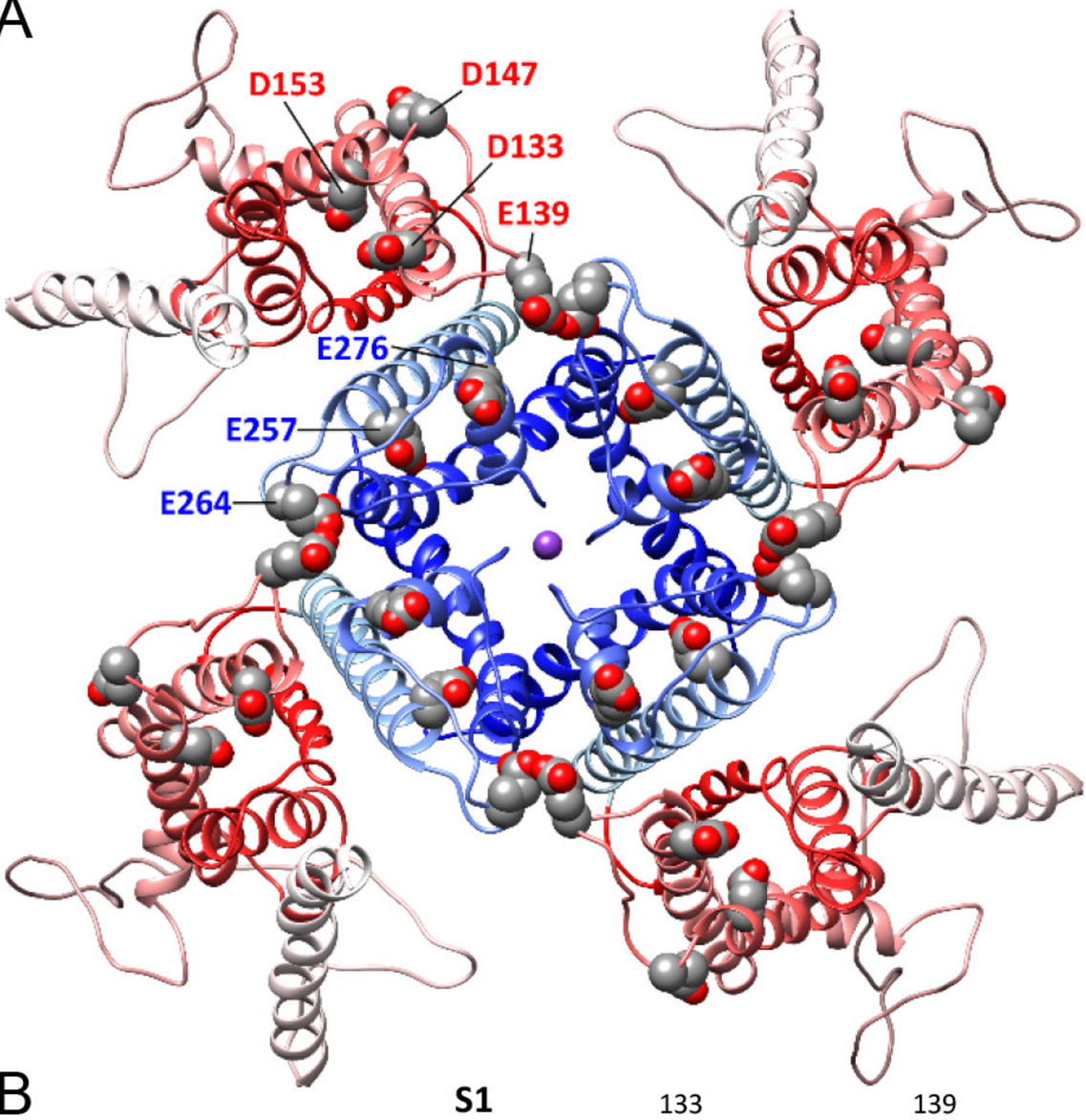

B

S1

```
                                                133                 139
mSlo1: RVLVVLVFALSIGALVIYFIDSSN--PIE:  139
aSlo1: RILVGLVFLLSIASLIIYFIDASTNTSVE:  128
Kv1.2: RIIAIVSVMVILISIVSFCLETLPI--FRD:  190
Shaker:RVVAIISVFVILLSIVIFCLETLPE--FKH:  254
Nav1.1:WFETF-IVFMILLSSGALAFEDIY--I--:  1231
Cav1.1:WFTNF-ILLFILLSSAALAAEDPI--RA-:  824
```

S2

```
          147       153
mSlo1: YKDFTLQIDMAFNVFFLLYFGLRFIAANDK:  174
aSlo1: SSSTTQQVDLAFNVFFMIYFFIRFVAANDK:  163
Kv1.2: FTDPFFIVETLCIIWFSFEFLVRFFACPSK:  247
Shaker:ITDPFFLIETLCIIWFTFELTVRFLACPNK:  304
Nav1.1:IKTMLEYADKVFTYIFILEMLLKWVAYGYQ:  1266
Cav1.1:RNQILKHFDIGFTSVFTVEIVLKMTTYGAF:  857
```

S5

```
                257                 264                 276
mSlo1: LTAAGFIHLVENSGDPWENFQNNQALTYWE:  276
aSlo1: LTAAGFLHLLENSGDPFFDFGNAQHLTYWE:  265
Kv1.2: FLFIGVILFSSAVYFAEADERDSQFPSIPD:  363
Shaker:FLFIGVVLFSSAVYFAEAGSENSFFKSIPD:  431
```

Pore helix

```
                292
mSlo1: CVYLLMVTMSTVGYGDVYAKTTLGRLFMVF:  306
aSlo1: CLYFLMVTMSTVGFGDIFATTVLGRTFVVI:  295
Kv1.2: AFWWAVVSMTTVGYGDMVPTTIGGKIVGSL:  393
Shaker:AFWWAVVTMTTVGYGDMTPVGVWGKIVGSL:  461
```

bioRxiv preprint doi: https://doi.org/10.1101/317339; this version posted May 8, 2018. The copyright holder for this preprint (which was not certified by peer review) is the author/funder, who has granted bioRxiv a license to display the preprint in perpetuity. It is made available under aCC-BY 4.0 International license.

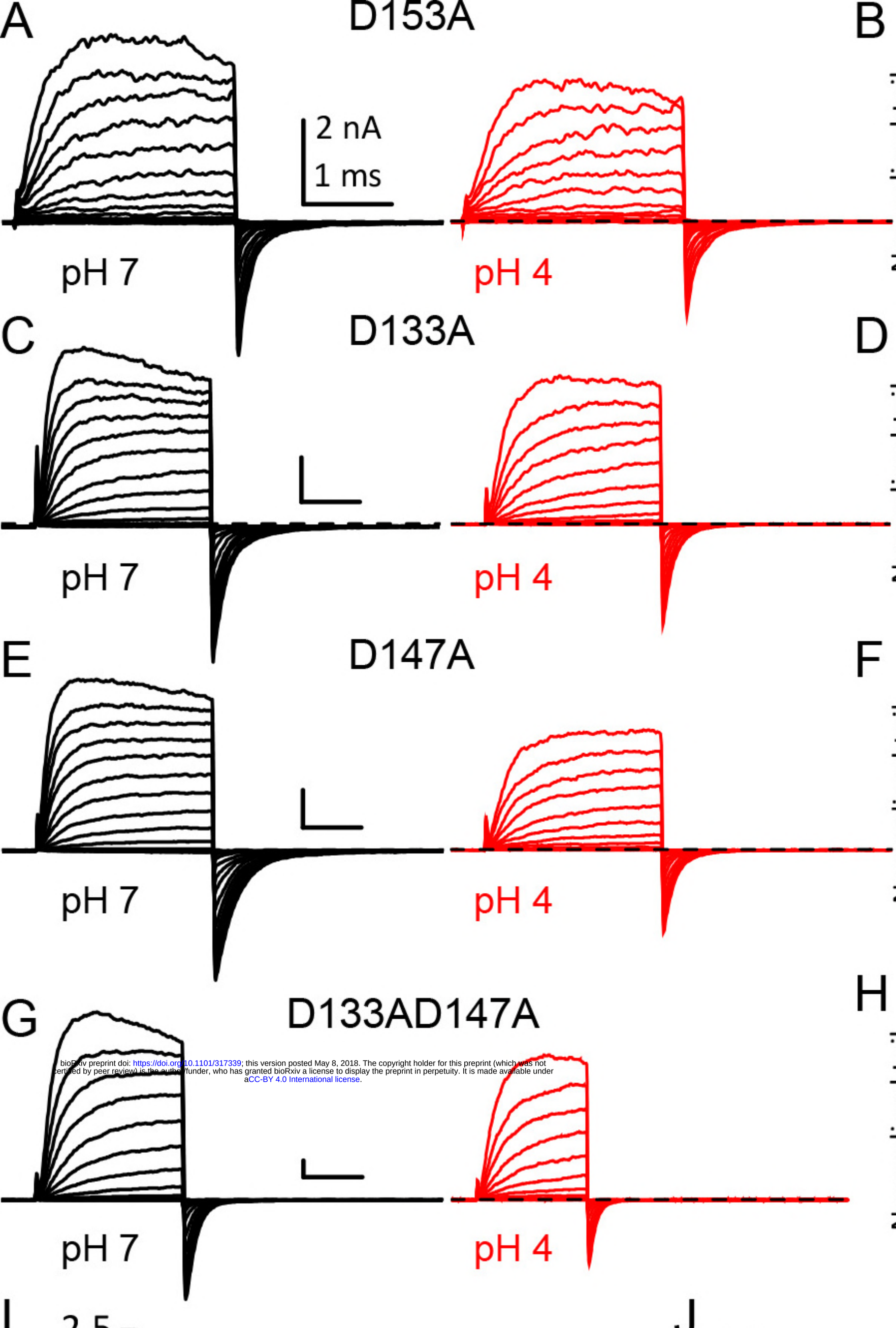

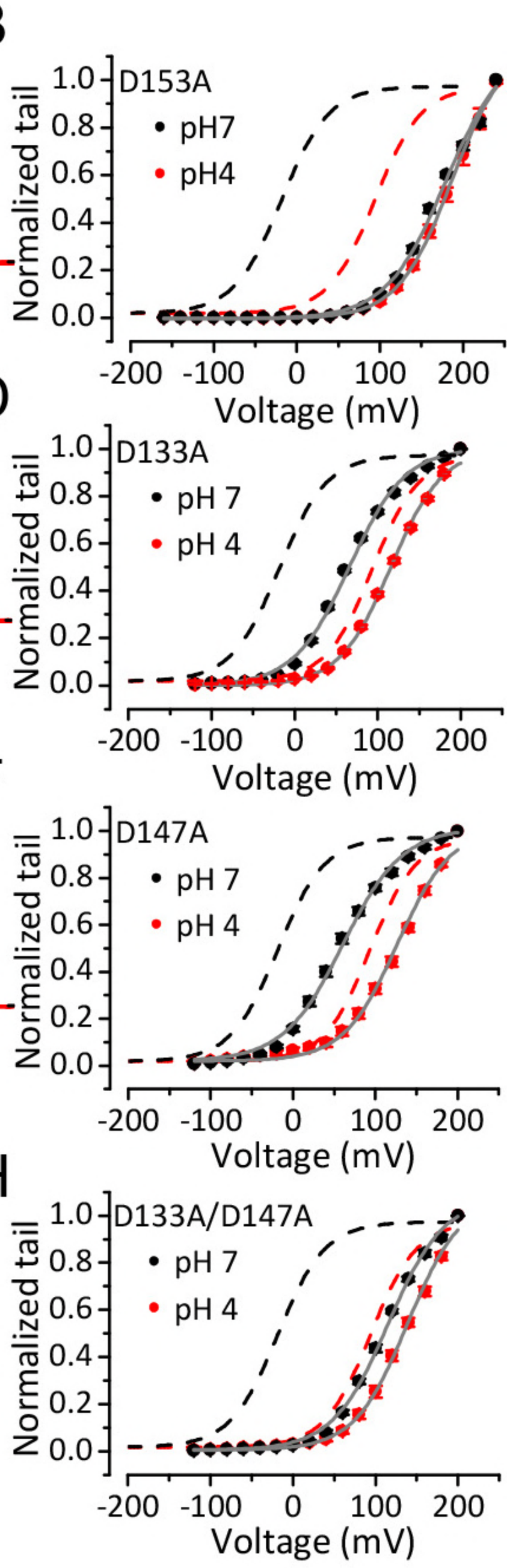

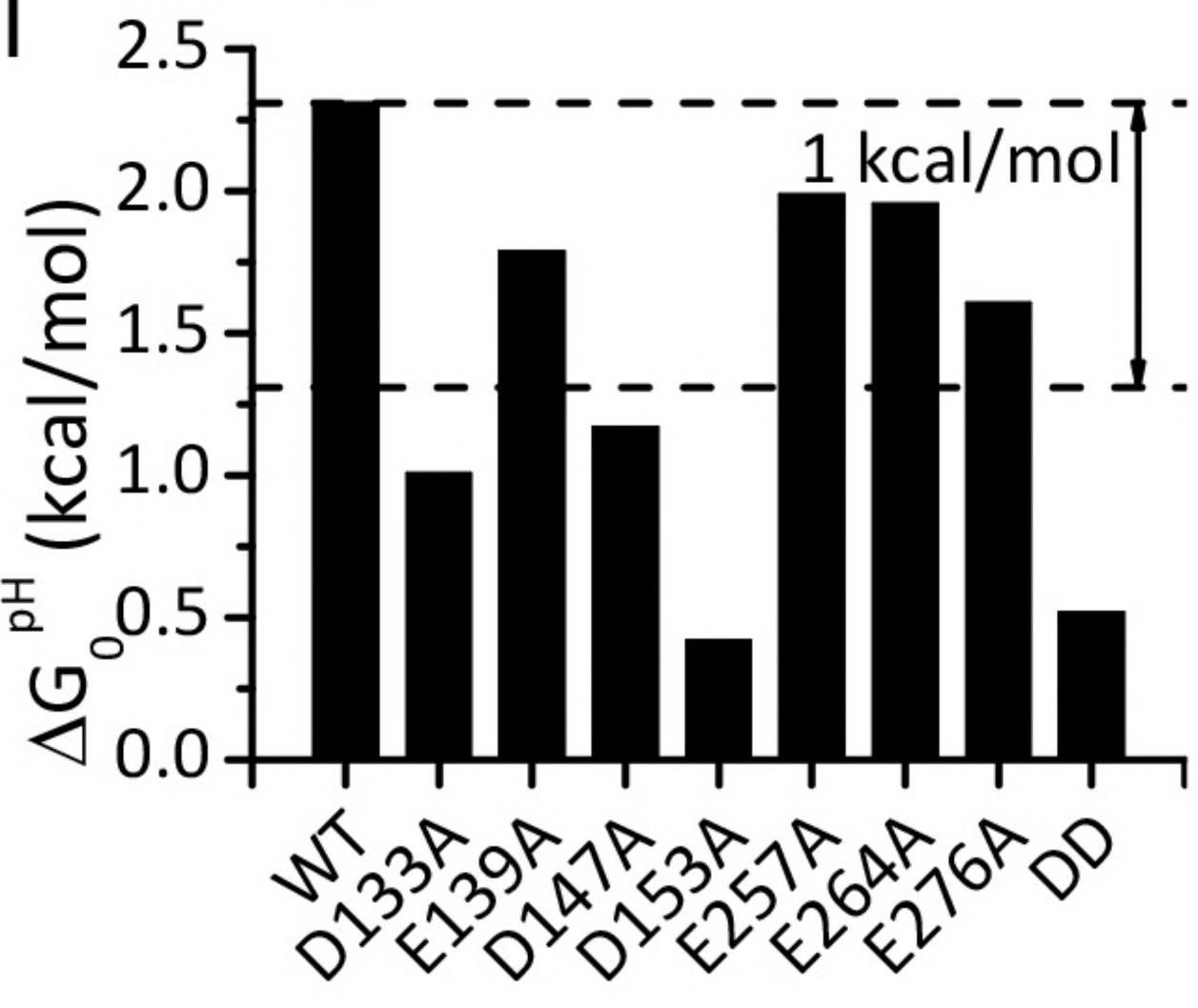

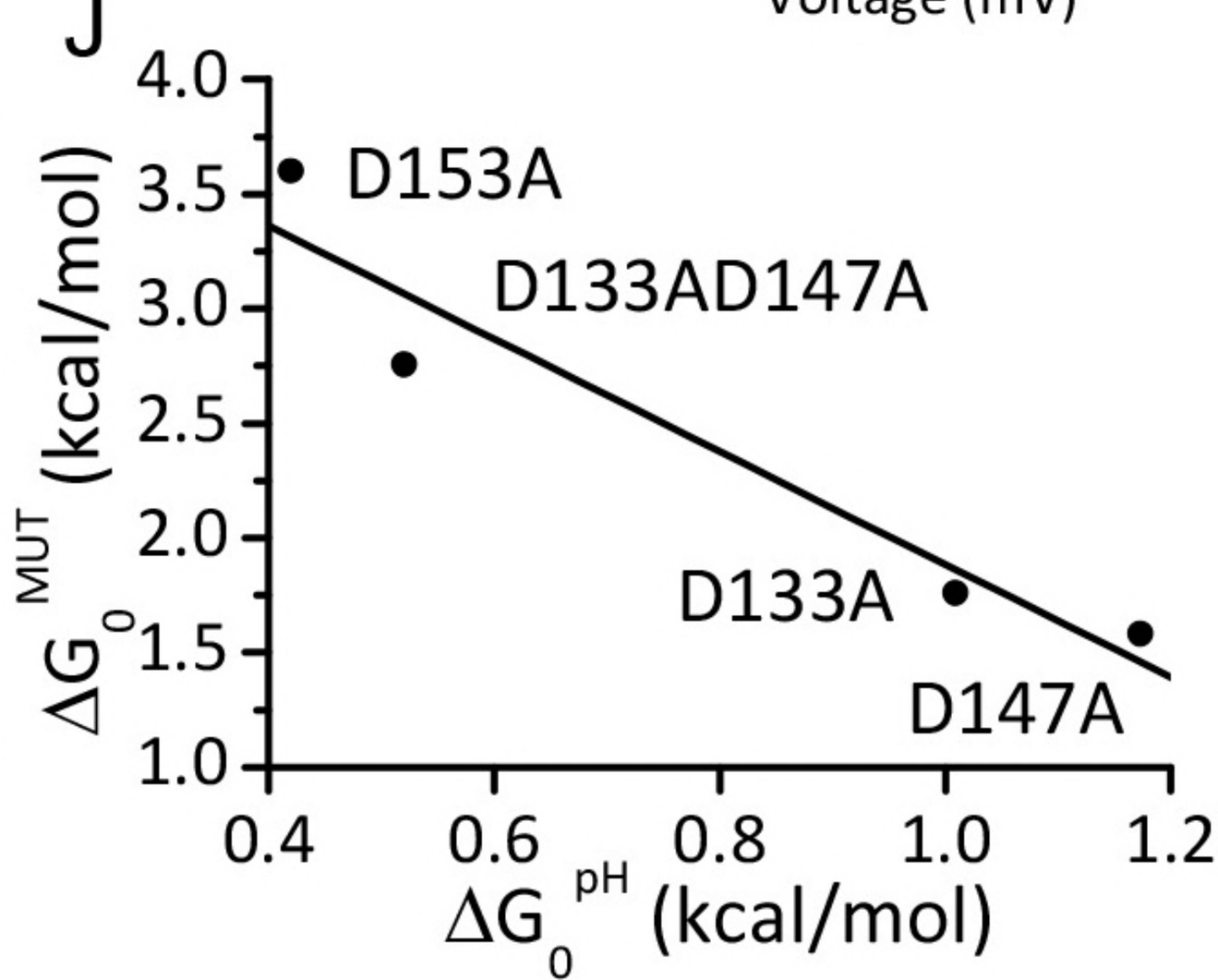

A

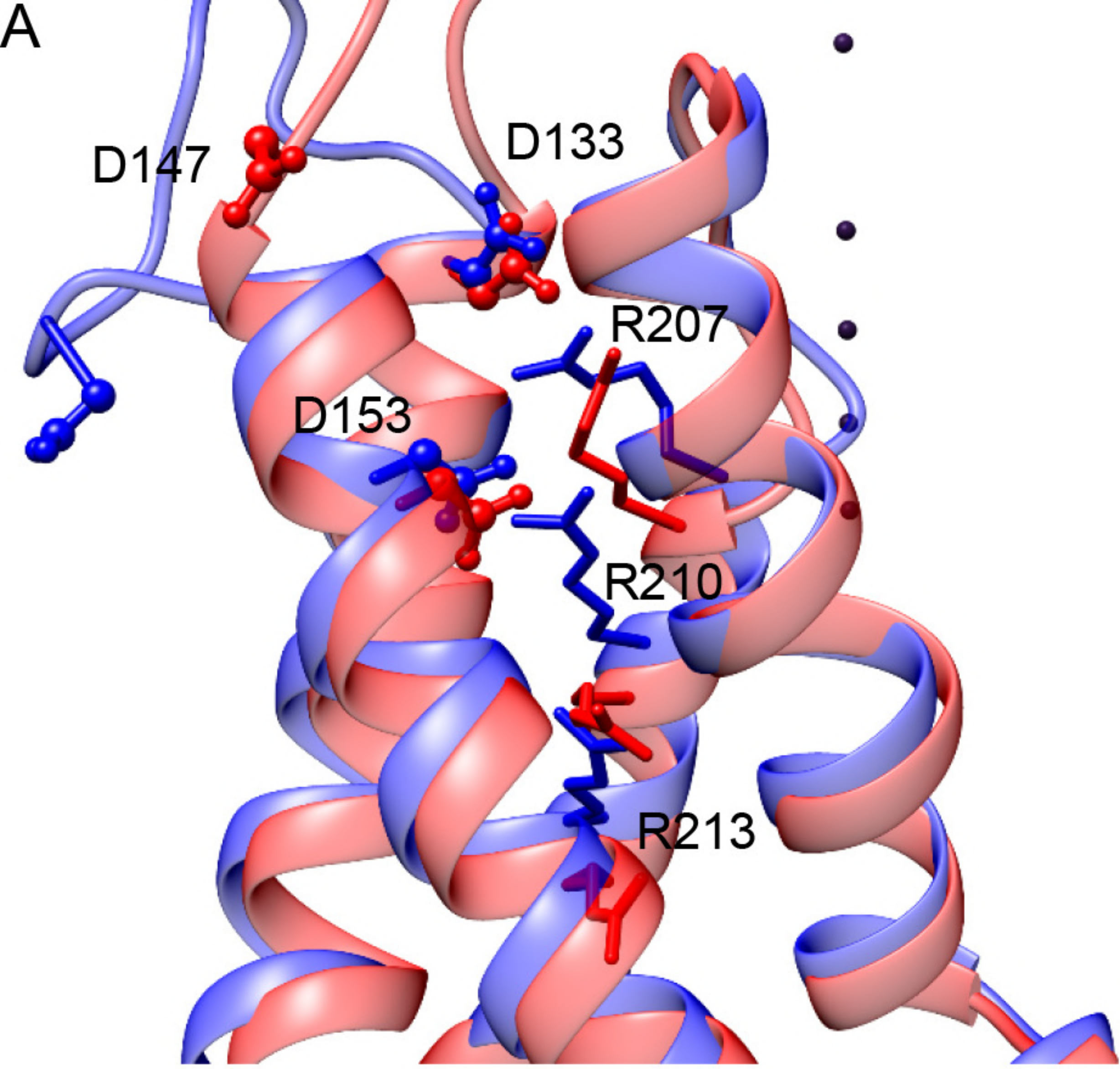

B Metal-free

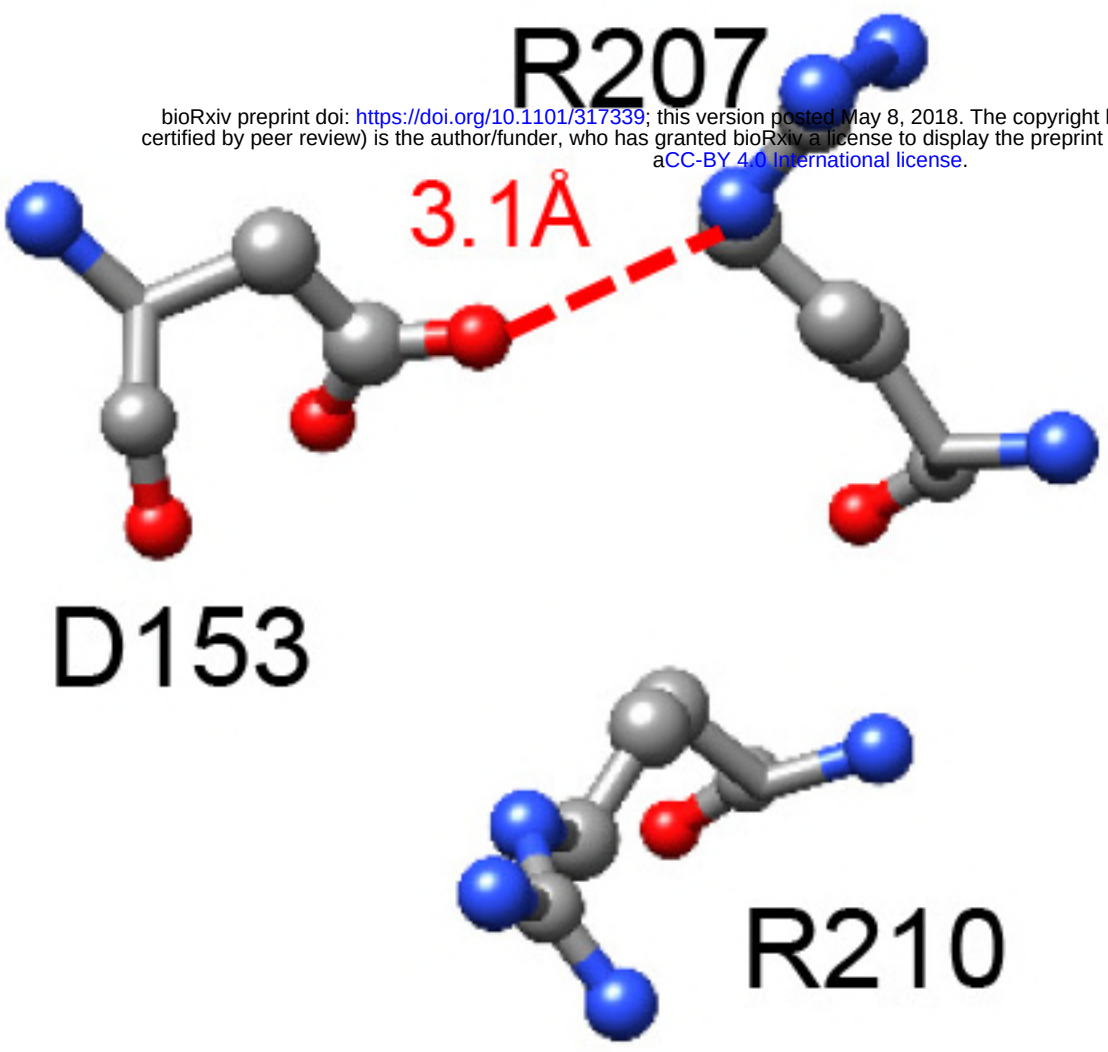

C Liganded

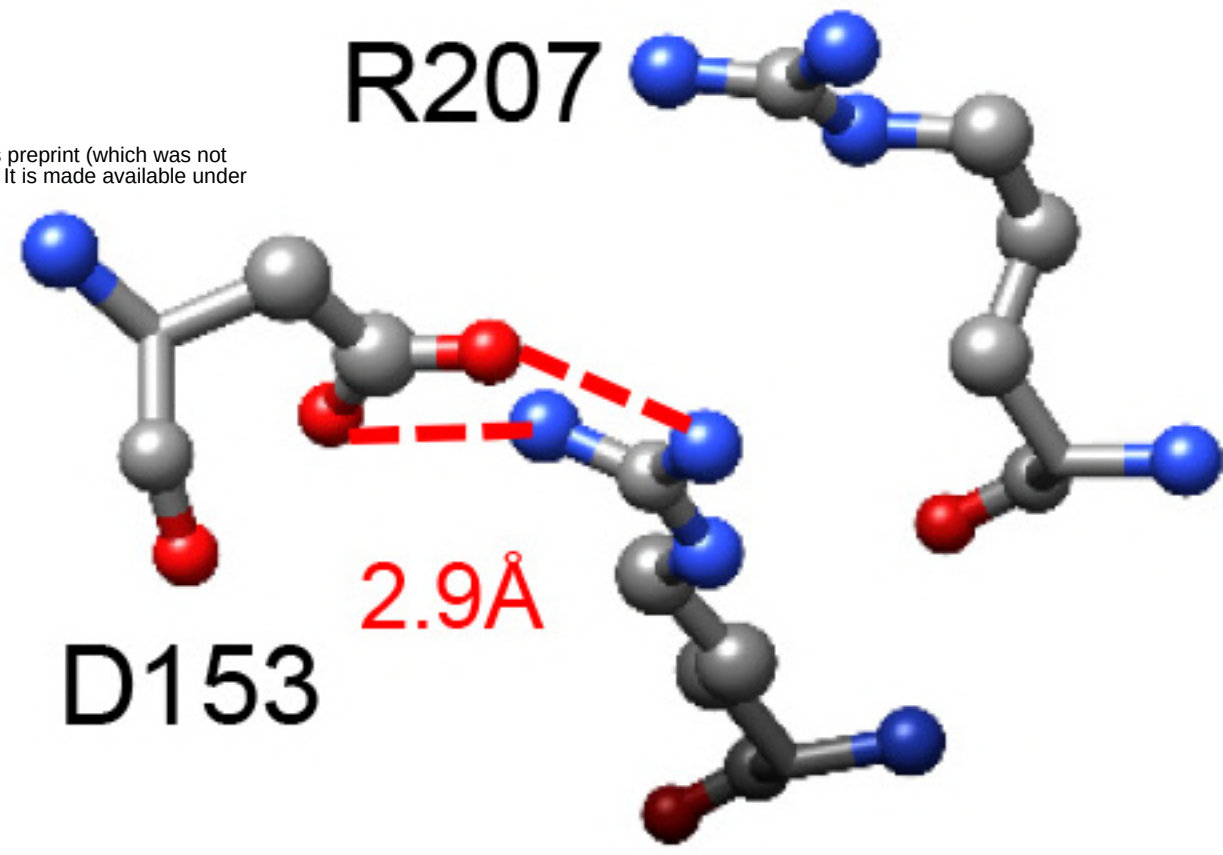

bioRxiv preprint doi: https://doi.org/10.1101/317339; this version posted May 8, 2018. The copyright holder for this preprint (which was not certified by peer review) is the author/funder, who has granted bioRxiv a license to display the preprint in perpetuity. It is made available under aCC-BY 4.0 International license.

D Metal-free

E Liganded